ESC European Society of Cardiology

European Heart Journal - Cardiovascular Imaging (2023) **00**, 1–21
https://doi.org/10.1093/ehjci/jead024

EACVI DOCUMENT

Multimodality imaging in thoracic aortic diseases: a clinical consensus statement from the European Association of Cardiovascular Imaging and the European Society of Cardiology working group on aorta and peripheral vascular diseases

Artur Evangelista[1]*, Marta Sitges [2,3], Guillaume Jondeau [4], Robin Nijveldt [5], Mauro Pepi [6], Hug Cuellar[7,8], Gianluca Pontone [9], Eduardo Bossone [10], Maarten Groenink[11], Marc R. Dweck[12], Jolien W. Roos-Hesselink[13,14], L. Mazzolai[15], Roland van Kimmenade[16], Victor Aboyans [17], and Jose Rodríguez-Palomares[1]

[1]Servei de Cardiologia, Hospital Vall d'Hebron, CIBERCV, Universitat Autonoma de Barcelona, Vall d´Hebron Research Institute, VHIR, Barcelona, Spain; [2]Cardiovascular Institute, Hospital Clinic, University of Barcelona, Villarroel 170, 08036 Barcelona, Spain; [3]CIBERCV, Institut Investigacions Biomèdiques August Pi i Sunyer (IDIBAPS), Villarroel 170, 08036 Barcelona, Spain; [4]Reference Center for Marfan Syndrome and related diseases, Cardiology Department, VASCERN HTAD European Reference Centre, Hopital Bichat, APHP, INSERM U1148, Université de Paris, France; [5]Department of Cardiology, Radboud University Nijmegen Medical Centre, Nijmegen, The Netherlands; [6]Centro Cardiologico Monzino IRCCS, Via Carlo Parea 4, Milano, Italy; [7]Radiology Department, Institut de Diagnòstic per la Imatge, Hospital Vall d'Hebron, Barcelona, Spain; [8]Universitat Autònoma de Barcelona, Vall d´Hebron Research Institute (VHIR), Barcelona, Spain; [9]Department of Perioperative Cardiology and Cardiovascular Imaging, Centro Cardiologico Monzino IRCCS, Milan, Italy; [10]Cardiology Division, Antonio Cardarelli Hospital, Via Antonio Cardarelli 9, 80131, Naples, Italy; [11]Department of Cardiology and Radiology, Amsterdam University Medical Center, Amsterdam, The Netherlands; [12]BHF Centre for Cardiovascular Science, University of Edinburgh, Chancellors Building, Little France Crescent, Edinburgh EH16 4SB, UK; [13]Cardiology Department, Erasmus MC, University Medical Center Rotterdam, Rotterdam, The Netherlands; [14]VASCERN HTAD European Reference Centre; [15]Division of Angiology, Centre Hospitalier Universitaire Vaudois, Lausanne, Switzerland; [16]Department of Cardiology, Radboud University Medical Center, Nijmegen, The Netherlands; and [17]Department of Cardiology, Dupuytren University Hospital, Inserm U1094, Limoges, France

Received 29 January 2023; accepted 30 January 2023

Imaging techniques play a pivotal role in the diagnosis, follow-up, and management of aortic diseases. Multimodality imaging provides complementary and essential information for this evaluation. Echocardiography, computed tomography, cardiovascular magnetic resonance, and nuclear imaging each have strengths and limitations in the assessment of the aorta. This consensus document aims to review the contribution, methodology, and indications of each technique for an adequate management of patients with thoracic aortic diseases. The abdominal aorta will be addressed elsewhere. While this document is exclusively focused on imaging, it is of most importance to highlight that regular imaging follow-up in patients with a diseased aorta is also an opportunity to check the patient's cardiovascular risk factors and particularly blood pressure control.

Keywords imaging • aorta • aortic syndrome • aortic aneurysm

Imaging modalities: methodology, advantages, and limitations

Transthoracic echocardiography

Transthoracic echocardiography (TTE) is used to measure the proximal aortic segments in routine clinical practice. However, by using all echocardiographic views, it is possible to visualize most aortic segments, if image quality is good (*Figure 1*; see Supplementary data online, *Video S1*). The aortic root and proximal ascending aorta are best imaged from the left parasternal long-axis view. To visualize the mid-distal ascending aorta, it may be necessary to move the transducer to upper intercostal spaces, while right parasternal views might help visualizing the distal portion of the ascending aorta. The proximal ascending aorta may also be visualized in the apical long-axis (apical three-chamber) and apical five-chamber views and even in modified subcostal views (especially in children). The aortic arch and the proximal descending aorta can be assessed from the suprasternal window. Moreover, the distal portion of the thoracic aorta can be observed in the parasternal long-axis view and in a modified apical two-chamber view while the

* Corresponding author. Tel: +34 932175153. E-mail: arturevangelistamasip@gmail.com

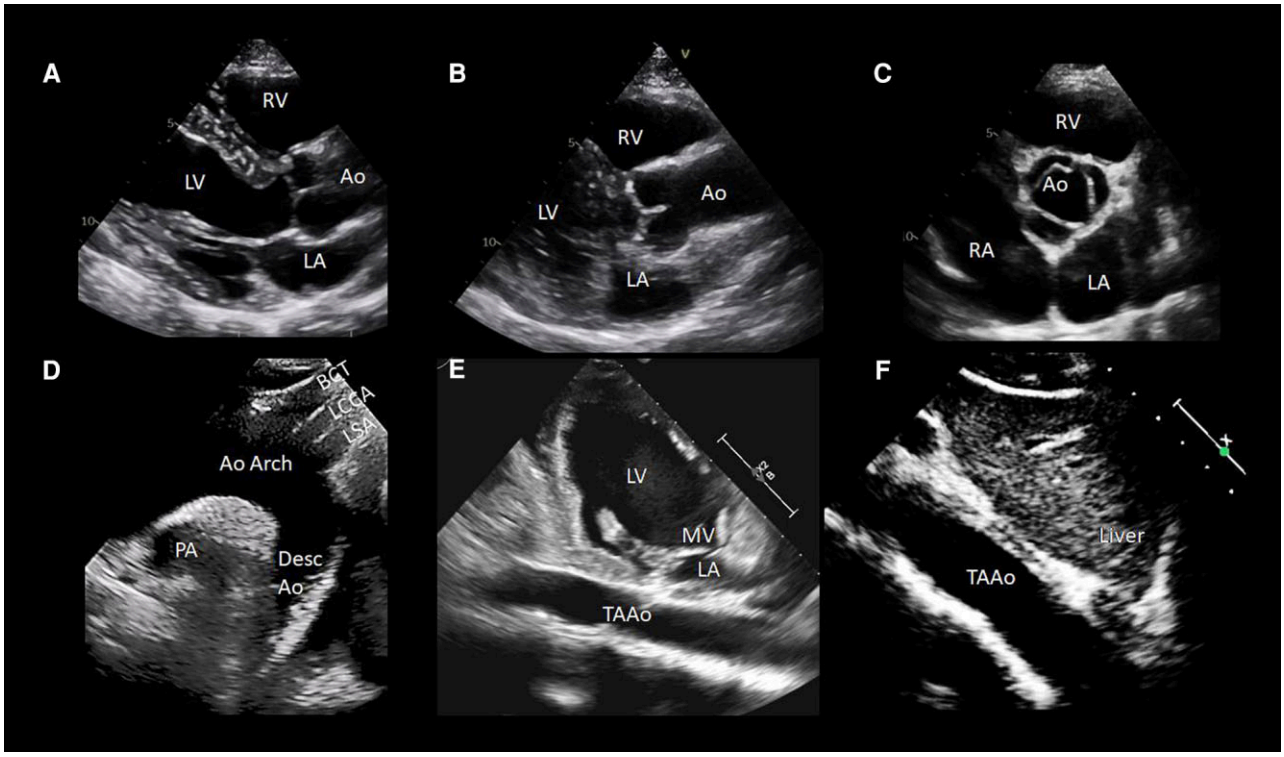

Figure 1 Transthoracic echocardiography of the aorta: the essential views. (*A*) standard parasternal long-axis view showing the Ao root and proximal ascending Ao; (*B*) adapted long-axis view of the entire ascending Ao from an upper parasternal view; (*C*) short-axis view of the aortic root and the aortic valve; (*D*) suprasternal view of the arch; (*E* and *F*) thoracoabdominal views of the Ao from the subxifoid and adapted 2-chamber view, respectively. Ao, aorta; BCT, barchiocephalic trunk; Desc Ao, descending Ao; LA, left atrium; LCCA, left common carotid artery; LSA, left subclavian artery; LV, left ventricle; MV, mitral valve; PA, pulmonary artery; RA, right atrium; RV, right ventricle; TAAo, thoracoabdominal Ao.

abdominal aorta is seen from subcostal and abdominal approaches. Finally, in cases with pleural effusion, the descending aorta may be imaged from the patient's back.[1–3] Three-dimensional (3D) probes allow for multiplanar views, potentially yielding more accurate measurements due to improved alignment of cutting planes.[4]

Transoesophageal echocardiography

The proximity of the oesophagus allows for high-resolution images of the thoracic aorta. The best views of the ascending aorta, aortic root, and valve are the long-axis (at 120–150°) and short-axis (at 30–60°) views (*Figure 2*). With the probe posteriorly oriented, short-axis or long-axis images of the whole descending thoracic aorta, from the upper segment to the coeliac trunk and the superior mesenteric artery, can be obtained. Although the take-off of the left subclavian artery is easy to visualize, the left common carotid and brachiocephalic arteries can be extremely difficult to image, usually requiring careful clockwise rotation of the probe. The distal portion of the ascending aorta and the proximal part of aortic arch are usually not visible (so-called 'blind spot'), because of the interposition of the trachea. The deep transgastric view can depict the aortic valve (AV) and the ascending aorta.[5]

Computed tomography

Computed tomography (CT) angiography, particularly with electrocardiogram (ECG) gating, is an essential tool to diagnose, to risk stratify, and to plan therapy in patients with thoracic aortic disease. Short acquisition times, widespread availability, high reproducibility, and the ability to provide simultaneous luminal and mural information of the whole thoracoabdominal aorta are its main strengths. It is of utmost importance to use an adequate protocol acquisition tailored to the clinical setting. CT protocols of the aorta typically include a non-contrast phase, an arterial phase as well as a late scan. The non-contrast phase allows for the assessment of aorta calcifications, intramural haematoma (IMH), and surgical material, the arterial phase describes the lumen, and the late phase may depict contrast leakage in the context of aortic dissection (AD) or prior endovascular repair.

ECG triggering is recommended to avoid motion artefacts of the aortic root and ascending aorta, which may impair size measurements or mimic AD, and allows also for the assessment of the coronary arteries. Pre-treatment with beta-blockers or ivabradine might be required to ensure adequate heart rates (below 80 bpm for CT angiographic scanning of the aorta), although this is less of a concern for the aorta compared with the coronary arteries when heart rate below 60 bpm is recommended. Two main methods of ECG synchronization are currently available: (i) ECG-gated spiral acquisition with data acquired throughout the entire cardiac cycle and retrospectively reconstructed, mainly recommended in emergency cases; (ii) ECG-triggered axial (sequential) acquisition, with lower radiation dose but more sensitive to heart rate irregularities.[6] Newer technologies such as dual-source and wide-detector CT systems overcome these limitations and can acquire the thoracic aorta in one or two heart beats, respectively.

Cardiovascular magnetic resonance

Cardiovascular magnetic resonance (CMR) is a reliable and reproducible imaging modality for aortic diseases, due to its capacity for

multiplanar and 3D imaging without the use of iodine-containing contrast agents or ionizing radiation. It is the ideal technique for comparative follow-up studies, especially in younger patients.

Technical aspects are also key when performing CMR to evaluate the aorta and should include ECG gating and acquisition at mid- or end-diastole to minimize motion artefacts. It is also of utmost importance to perform 3D imaging. CMR angiography (MRA) of the aorta with contrast-enhanced sequences often shows motion artefacts in the aortic root and is therefore less clinically useful at this location; however, this approach yields highly reliable measurements of the aorta lumen beyond the aortic root.[7] Post-processed 3D volume-rendered images can clarify complex congenital anatomy of the aorta and great vessels. 3D non-contrast-enhanced MRA sequences can substitute contrast-enhanced MRA for morphologic follow-up of the thoracic aorta. Nevertheless, contrast-enhanced MRA is recommended for the whole thoracoabdominal aorta.

Additionally, 2D turbo spin echo sequences (so-called black blood images) may be useful for assessing aorta wall abnormalities, such as IMH (hyperintense on T1-weighted image and isointense on T2-weighted image in the subacute phase), aortitis (hyperintense on T2-weighted images), and atherosclerotic plaques and thrombi (isointense on both T1-weighted and T2-weighted images). Cine steady-state free precession (SSFP) imaging is recommended for assessing AV morphology and function. CMR also allows for the evaluation of aorta biomechanical parameters such as stiffness, distensibility, and strain, used to assess aorta elasticity in patients with Marfan syndrome, bicuspid AV (BAV), or aorta aneurysms. Aorta stiffness by pulse wave velocity (PWV) defined by phase-contrast sequences has been associated with the severity of atherosclerotic disease and the occurrence of cardiovascular events. In patients with BAV, aortic stiffness is similar to that described in the normal population whereas Marfan syndrome patients have a stiffer aorta.[8] 2D phase-contrast velocity mapping is part of the standard examination and allows flow assessment and quantification of associated AV stenosis and regurgitation, evaluation of flow patterns in the true and false lumen (FL) of AD, and estimation of pressure gradients across a coarctation and its collateral flow.[9]

In recent years, 3D-cine (time-resolved) phase-contrast CMR with three-directional velocity encoding (4D-flow) has been developed to study intravascular flow[10] (*Figure 3*; see Supplementary data online, *Video S2*). It quantifies flow similarly to 2D-cine phase-contrast CMR, has good scan repeatability, and allows for the analysis of advanced parameters such as wall shear stress (WSS) or turbulent kinetic energy. In patients with BAV, these sequences have added an understanding of the complex flow patterns distal to the AV, shedding light into a potential mechanism underlying associated aortic dilation. Using 4D-flow or image-based computational modelling, elevated WSS has been associated with aortic wall degradation in ascending thoracic aortic aneurysms.

Positron emission tomography

Molecular imaging with positron emission tomography (PET) allows for the non-invasive assessments of metabolic activity in the cardiovascular system. While novel tracers targeting calcification, fibrosis, and thrombus formation are emerging, most PET studies have focused on inflammatory activity in the aorta of patients with large vessel vasculitis. These provide important diagnostic information and the potential ability to track changes in disease activity over time and with therapy. Limitations to the technique include radiation exposure and the relatively high costs and limited availability of cardiovascular PET scanners.[11]

Key point 1. TTE permits adequate assessment of several aortic segments, particularly the aortic root and proximal ascending aorta. However, CT provides rapid, accurate, and reproducible assessment of the entire aorta. In addition, CMR offers morphologic, functional, and tissue characterization information without radiation exposure. PET is used to diagnose inflammatory or infectious disease of the aorta.

How to measure the aorta

Accurate measurements of the maximal diameter of the aorta are key to establish a diagnosis of aorta dilation, to assess disease progression, and most importantly to guide the need for prophylactic intervention according to current guidelines.[12] Given the known variability in measurements of aorta diameter, mainly related to the different methodologies and imaging modalities used, it is of utmost importance to follow standardized measurement techniques. One of the main goals of the present expert consensus is to provide such standardization. Some general rules can be proposed as the basis for measurements of the aorta diameter.

(a) When using echocardiography, measurements of the aorta diameter should be made with the leading-to-leading edge method (*Figure 4*). Because of the axial resolution of ultrasound, the thickness of the aortic wall is falsely increased by ~1–2 additional mm[13,14] (the real thickness of the aortic wall as measured by CT is typically 1 mm). Consequently, measurement of the aortic diameter with echocardiography (using the inner-to-inner convention) systematically underestimates the aorta diameter measured by CT. This technical artefact happens in all segments of the aorta, not only the ascending aorta. All aorta diameter measurements should be made in diastole. Systole is associated with expansion of the aorta of ~2 mm.[15] Several authors have demonstrated optimal agreement using leading edge echo measurement and inner-to-inner CT/CMR measurement in end-diastole.[14,16,17] Additionally, most of the echocardiographic studies that demonstrated the benefits of prophylactic surgery were performed using this convention.

(b) When the aorta wall is thickened due to the presence of atheroma, IMH, or aortitis, outer-to-outer diameter (including the aorta walls) should be also reported.

(c) In the presence of intraluminal thrombus, the inner-to-inner measurement should exclude the thrombus (*Figure 5*). If the thrombus is circumferential, the outer-to-outer convention must be used instead.

(d) In AD, the inner-to-inner diameter should include both the true and FL. If the FL is partially or totally thrombosed, indication in (c). should be applied.

Beyond these general recommendations, each segment of the aorta has its own individual considerations that are addressed specifically below.

The thoracic aorta consists of four parts, which can be further subdivided:

- The aortic root consists of the annulus, the valvular cusps, and the sinuses of Valsalva.
- The tubular segment of the ascending aorta corresponds to the segment from the sinotubular junction to the origin of the brachiocephalic artery.
- The aortic arch is defined from the brachiocephalic artery up to the aortic isthmus.
- The descending aorta is from the isthmus to the diaphragm.

The aortic root

The most difficult segment to measure is the aortic root, given that it has a non-circular shape. This applies also to the AV annulus, particularly important for transcatheter AV implantation, but this is beyond the topic of this expert consensus. Diameters measured using CT/CMR from sinus-to-sinus are generally 2 mm larger on average than those

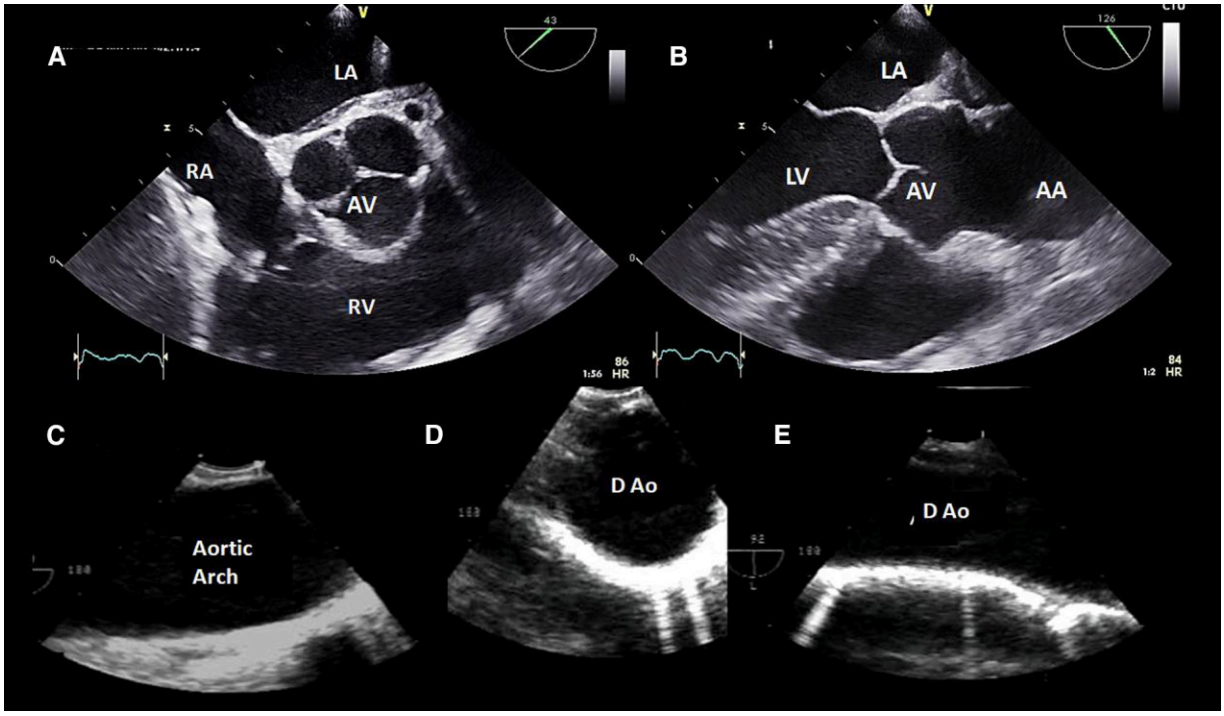

Figure 2 Transoesopahgeal echocardiography of the aorta: the essential views. (*A*) short-axis view (30–40°) of the aortic valve at the level of the great vessels; (*B*) long-axis view of the ascending aorta (130–140°) showing the aortic sinuses, the sinotubular junction and the tubular ascending aorta; (*C*) longitudinal view of the aortic arch; (*D*) short-axis view of the descending thoracic aorta (0°); and (*E*) long-axis view of the descending thoracic aorta (90°). AA, ascending aorta; AV, aortic valve; D Ao, descending thoracic aorta; LA, left atrium; LV, left ventricle; RA, right atrium; RV, right ventricle.

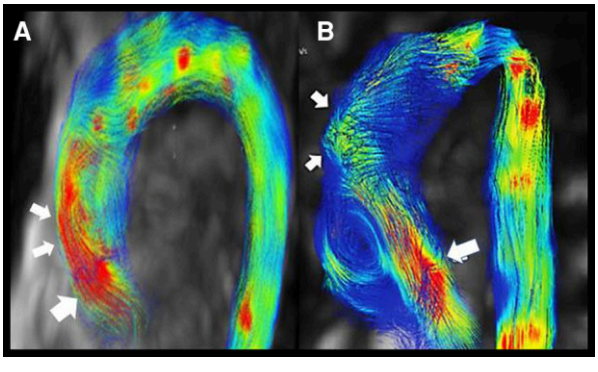

Figure 3 Systolic 3D streamline representation of 4D-flow CMR data. Two different patients with a bicuspid aortic valve: (*A*) right-left cusp fusion and (*B*) right non-cusp fusion. Notice the difference in the flow direction: in right-left cusp fusion, flow impinges on the outer curvature of the proximal ascending aorta (arrows), including the root (large arrow). In right non-cusp fusion, flow is posteriorly directed in the proximal aorta (large arrow) and impinges on the outer wall in the distal ascending aorta (arrows). See also Supplementary data online, *Video S2*.

measured from sinus-to-commissure (*Figure 4*). The sinus-to-sinus method has several advantages, including the ease of detecting cusp margins in co-axial CT/CMR views, the close agreement with 2D echocardiographic measurements, and its greater feasibility in patients with BAV.[14,16,18] Therefore, the consensus is that the maximum aortic root diameter by CT/CMR must be determined in a transversal plane with double obliquity measuring the diameter from sinus to sinus at end-diastole, using the inner-edge-to-inner-edge convention.

By echocardiography, the diameter of the sinus of Valsalva is typically measured from long-axis parasternal views with specific focus on obtaining a view of the central line of the aorta. Studies comparing the maximum aorta root diameter obtained by CT and echocardiography

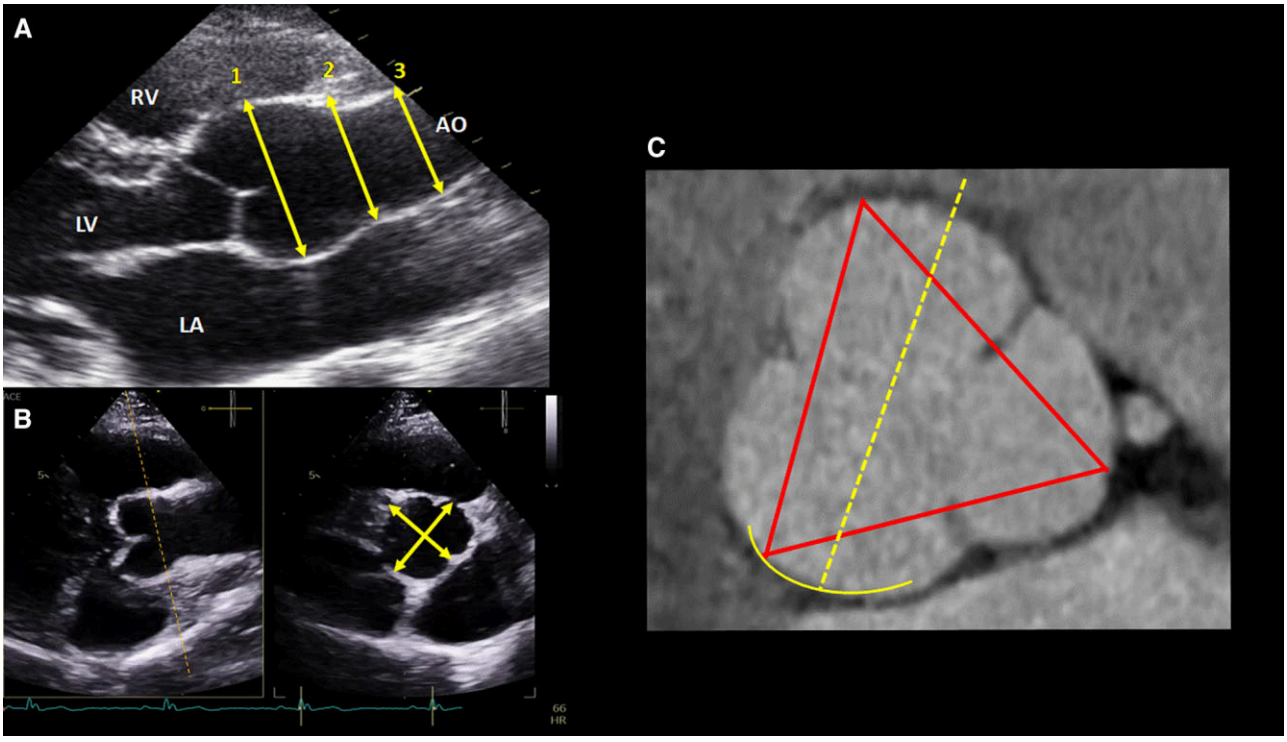

Figure 4 How to measure the aorta. (*A*) Parasternal long-axis view by transthoracic echocardiography illustrating measurement of aortic root (1), sinotubular junction (2) and proximal ascending aorta (3) diameters at end-diastole using the leading edge-to-leading edge method; (*B*) 3D echocardiography from the parasternal long-axis view using orthogonal views (biplane or x-views) allows for a better alignment and measurement of the aortic root diameters (yellow arrows); (*C*) aortic root cusp-to-cusp diameters measured by cardiac CT at end-diastole using the inner-to-inner convention (red lines), in yellow the representation of the direction of ultrasound beam that would be projected by parasternal long-axis view echocardiography.

have concluded that echocardiographic measurements from the left parasternal long-axis view using leading-to-leading edge are concordant to sinus-to-sinus inner-to-inner edge measurements taken with CT/CMR.[14,16,17]

Short axis parasternal echocardiographic views are inappropriate as perpendicular planes cannot be ensured and the lower lateral resolution of ultrasound limits accurate measurements of the aortic walls and edges. However, 3D echocardiography may partially overcome this limitation as multiplane views [multiplanar reconstruction (MPR) or biplane views] allow for accurate perpendicular views and true short-axis, transversal views of the aortic root.[4] Despite initial promise, more validation studies are still needed on the potential role of 3D echocardiography particularly multiplane echocardiography, in assessing this asymmetry and improving the accuracy of the measurement of the largest diameter of the aortic root (*Figure 4*).

Of note, it is also important to address the asymmetry of the aortic root that might yield different diameters between aortic sinuses. This is the case for patients with BAV and for those with localized dilation of the non-coronary sinus, the most frequently dilated sinus. Significantly asymmetric root dilatation, defined with more than 5 mm difference in oblique diameters, can be present in up to >40% of patients with BAV (particularly in those with fusion of the right coronary and non-coronary cusps and those without raphe).[19,20] In a BAV with two sinuses, two orthogonal diameters, the longitudinal and transverse diameters, should be measured (*Figure 6*). Therefore, considering that significant asymmetry of the aortic root is very prevalent, when aortic root dilation is initially diagnosed by echocardiography, a multiplanar CT/CMR scan is recommended at least as a baseline reference and confirmatory examination of the echocardiographic measurements. In case of asymmetric dilation of the aortic root, the recommendation is also to report the three sinus-to-sinus diameters measured for each patient particularly during follow-up.

Tubular segment of ascending aorta

Maximum diameter measurements in the tubular portion of the ascending aorta and indeed of the rest of the aorta are easier due to its more typical cylindrical shape. By echocardiography, the tubular ascending aorta is usually measured from long-axis parasternal views at end-diastole. As mentioned above, to evaluate optimally the medium-upper part of the ascending aorta and to scan it on its central axis, it is recommended to move the transducer up one or two intercostal spaces. Using CT/CMR, maximum aortic diameter should be measured from inner-to-inner edges at diastole on double oblique images reconstructed at the most dilated level of the aortic segment. The presence of significant atherosclerosis, IMH, or aortitis may limit accuracy. In these cases, the outer-to-outer diameter should also be reported (*Figure 5*). The most dilated level of the ascending aorta is frequently at the pulmonary trunk, but that is patient and pathology dependent. Both maximum anteroposterior diameter and a perpendicular diameter should be measured, but if the aortic shape is circular, they should be identical, and a single value can then be reported

Aortic arch and descending thoracic aorta

In patients with good acoustic window, echocardiography may be useful to screen for aortic arch dilation but has low accuracy and

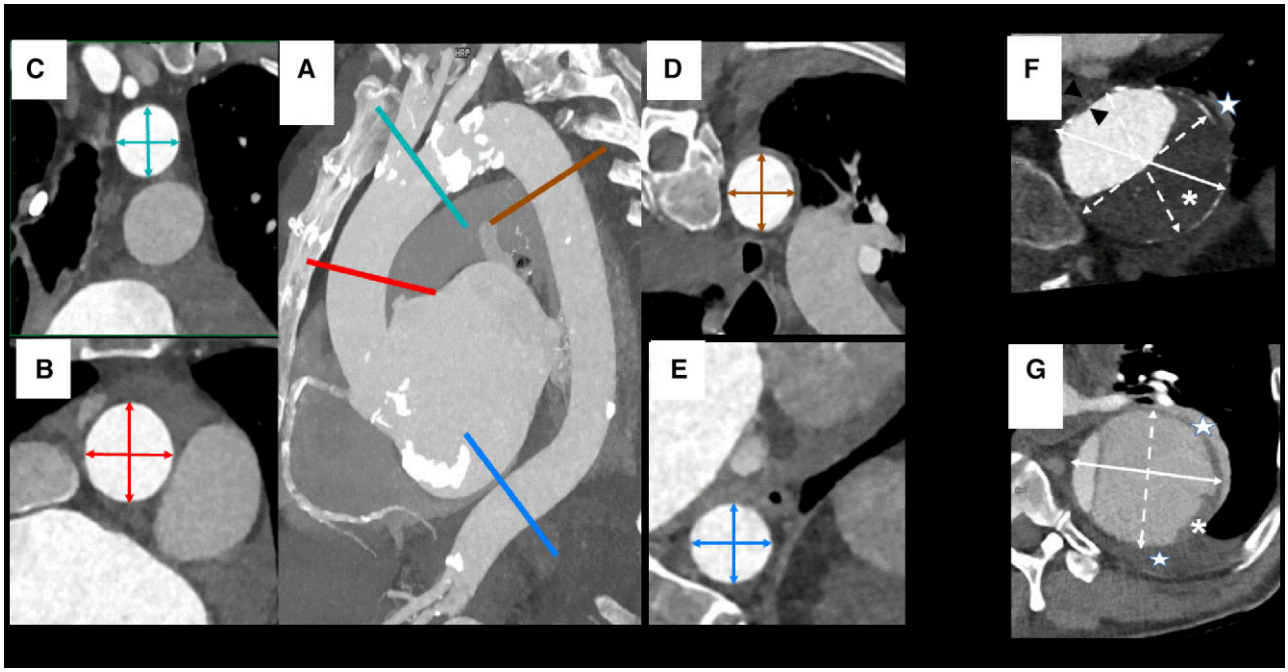

Figure 5 How to measure the aorta in CT. (*A*) Sagittal maximum intensity projection of an ECG-gated CT angiography shows an elongated thoracic aorta in an elderly patient. Measurements in the patient's axial plane would result in overestimation of the maximum distance. Coloured lines show alignment of the cutting plane of multiplanar reconstructions for each aortic segment depicted in *Panels B–E*. (*B–E*) Double oblique multiplanar reconstructions of the ascending aorta (*B*), arch (*C*), proximal descending (*D*), and distal/retrocrural aorta (*E*) with measurements of maximum inner-to-inner distance and its orthogonal distance. In non-pathologic segments and fusiform dilatation, both distances should be similar and can be averaged. (*F*) Double oblique multiplanar reconstruction of a fusiform aneurysm of the descending thoracic aorta, with significant thickening of the aortic wall due to the combination of an atherosclerotic plaque (black arrows) and a large intraluminal thrombus (white asterisk) at its posterolateral aspect. The maximum outer-to-outer distance (solid white arrow) is reported, as well as the maximum wall thickness. Periaortic fat and lung collapse (white stars) should not be included in the measurement. Alternative diameters (dotted white arrows) are marginally shorter. (*G*) Double oblique multiplanar reconstruction of the dissected descending thoracic aorta at its most dilated segment. The maximum inner-to-inner distance bisects the centre of the flap (solid white arrow) and includes the intraluminal thrombus (white asterisk). The longest orthogonal distance (dotted white arrow) can also be reported. Lung collapse and pleural effusion are excluded (white stars).

reproducibility when taking diameter measurements at this level and particularly in the descending aorta. Transoesophageal echocardiography (TOE) may be better for this purpose than TTE; however, it may be hard to get in to a co-axial transverse plane, and regular follow-up using this method is uncomfortable. CT and CMR are therefore the preferred and recommended imaging modalities. Using these imaging modalities, the aortic diameter should be performed using the inner-to-inner edge method. Whenever wall thickening, thrombus or dissection flaps are present, the outer-to-outer edge diameter should be additionally reported as previously mentioned. In these aorta segments, it is particularly important to avoid off-axis imaging that can overestimate the aortic diameter in patients with tortuous aorta courses. Therefore, adequate MPRs with CT/CMR should be warranted.

Key point 2. Maximum aortic diameter should be measured at end-diastole using the leading-to-leading edge convention on echocardiography and the inner-to-inner edge convention on CT/CMR using transverse planes with double obliquity.

Key point 3. Because the true central axis of the aorta can be sometimes difficult to find when using TTE, assessment of the aortic diameter by CT/CMR is always mandatory before taking any decision for intervention.

Normal aorta diameter values

Reported reference maximum normal aortic diameters values at different segments of the aorta are shown in *Figure* 7. Factors influencing the aorta size in the normal population include age, gender, ethnicity body surface area (BSA) and particularly, height.[21]

In the specific case of genetic aortopathies where dilation may be a major diagnostic criterion, *Z*-scores should be used to determine if aorta dilation is present. The *Z*-score is the number of SDs above or below the predicted mean normal diameter. Therefore, an aortic diameter can be considered normal when the *Z*-score is ≤ 2. In infants, aorta dilation must be differentiated from aorta growth, proportional to BSA, and within normal paediatric reference values. Blood pressure and genetic factors are also determinants, even in the normal population. In this regard, the rate of growth in the size of the aorta in adults is about 0.9 mm in males and 0.7 mm in females per decade, because of loss of the elastic properties of the media. When body mass index is on the low or the high range, we recommend using nomograms to report the aortic diameter. Supplementary data online, *Table S1* summarizes

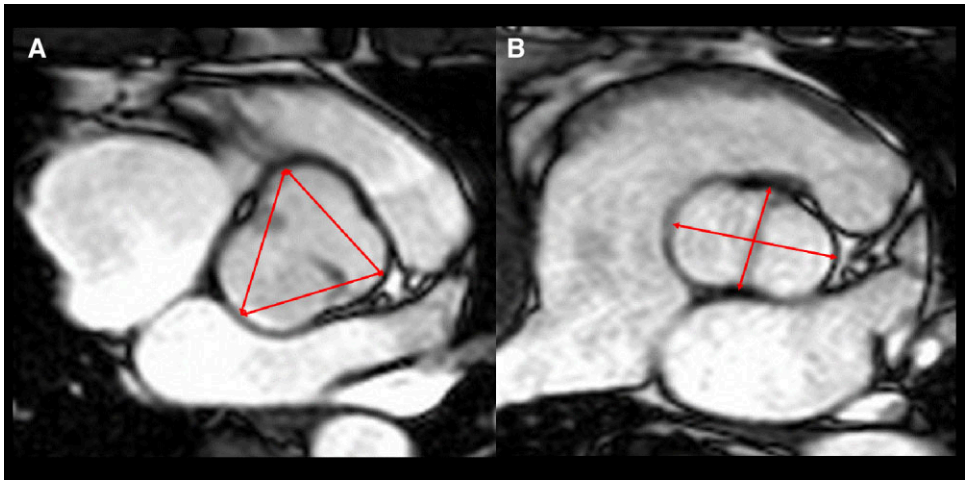

Figure 6 How to measure the aortic root in bicuspid aortic valve (BAV). SSFP cine CMR sequence at the level of the aortic valve in two different patients with a BAV: (*A*) patient with a fused type BAV (right-left type fusion). (*B*) Two-sinus type (latero-lateral phenotype). The red arrows show the different conventions used to measure the sinuses of Valsalva: (*A*) cusp-to-cusp convention, (*B*) maximum longitudinal diameter and a perpendicular one.

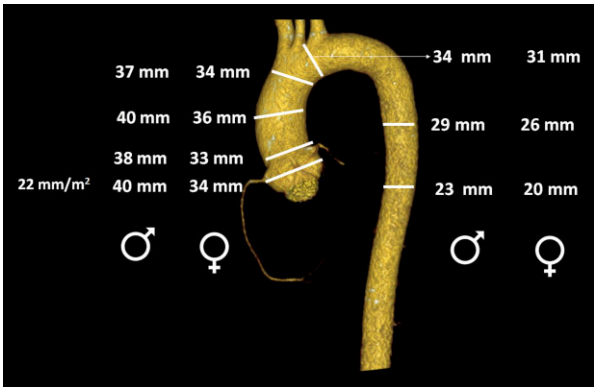

Figure 7 Maximum diameter reference values for different segments of the aorta according to gender but without normalization by age and body size.[15,21–23] See other references in Supplementary data online.

the most widely used and recommended nomograms that were developed for echocardiography but are also used for CT and CMR.[22,24]

Key point 4. Factors influencing the aorta size in the normal population include age, gender, ethnicity, BSA, and particularly, height. In routine clinical practice, a diameter of the aorta >40 mm in male and >34 mm in female adults or an indexed diameter/BSA > 22 mm/m^2 usually indicate aorta dilation.

Aortic dilation

Definition

Although aorta dilation is defined by an aorta diameter >2 SD of the mean normalized by age, gender, and body size (>2 *Z*-score), in routine clinical practice, a diameter of the aorta >40 mm in male adults and >34 mm in female adults or an indexed diameter/BSA > 22 mm/m^2 usually indicates aorta dilation. The term aneurysm was classically defined as an aorta diameter >50% the normal value. Since in many cases of ascending aorta dilation, the surgical indication is established before achieving this diameter in agreement with the current guidelines,[12] we strongly recommend the use of significant aorta dilation specifying the diameter value while using the term aneurysm when the diameter of the ascending aorta is >45 mm. This cut-off value is arbitrary and based on the fact that it implies a significant and clinically relevant aortic dilation. In addition, aorta dilation may adopt specific geometries altering the shape of the aorta that can be classified as fusiform or saccular. These abnormal shapes are frequently better defined with 3D imaging modalities.

Risk of complications

The relationship between the aorta diameter and the risk of dissection/rupture is well-established with lower thresholds in genetic diseases

(including some BAV)[25] than acquired aortic diseases, as outlined in more detail in the current guidelines.[12] This evidence underscores the importance of accurate measurements of the maximum aorta diameter with imaging. The risk of dissection or rupture is also related to the growth rate or progression of the aorta dilation, which warrants periodic surveillance with imaging after the initial diagnosis of aorta dilation.[12] This highlights the importance of the reproducibility of aorta diameter measurements. Aorta tortuosity might be another parameter to consider in clinical decision making, in particular in patients with borderline indications for surgery and genetic aortopathies.[26] Finally, imaging of the aortic branches, looking for dilation/dissections in mid-sized arteries, is particularly recommended in some genetic aortopathies [related to variants in the transforming growth factor beta pathway and possibly FBN1], as these abnormalities appear associated with poor outcomes.[27] Other imaging parameters proposed as predictors of rapid aorta enlargement or events include effacement of the sinotubular junction, aorta wall stiffness, molecular assessments of disease activity, and blood flow pattern. However, data supporting their predictive value are much more scarce and still controversial.

Follow-up: how and when

The ideal imaging modality used for the follow-up of adults with aorta dilation should be as reproducible, accurate and widely available as possible because repeated exams are required over time. To reduce variability, the same imaging modality should always be used over time. In this sense, TTE stands as the preferred imaging modality to follow-up patients with dilation of the aortic root or ascending aorta, where these segments are well visualized on echocardiographic windows. In patients with a dilated aorta, baseline aorta diameters at the time of diagnosis should be validated with CT or CMR. Once the agreement between the aorta dimensions measured by TTE and CT/CMR has been confirmed, TTE can be used for serial imaging of the dilated aortic root and the proximal ascending aorta. Conversely, if aorta diameters obtained from TTE and CT/CMR differ by more than 3 mm from echocardiographic diameters, follow-up should be based on CT/CMR. When dilation involves the distal (upper) portion of the ascending aorta, the arch, or the descending thoracic aorta, CT and CMR are the recommended imaging modalities for follow-up (*Figure 8*).

Follow-up intervals between imaging exams will be slightly different depending on the predicted growth rate of the dilated aorta. Generally, when baseline aorta diameter is >45 mm, a second exam is recommended 6 months after the initial diagnosis to confirm stability/progression of the aorta dilation. Thereafter, serial exams can proceed on a yearly basis.[28] If a real increase in aortic diameter or in the annual growth rate is confirmed, the time intervals for follow-up should be reduced. Conversely, stability in aortic diameters measured over a period of years might eventually lengthen these follow-up intervals. In particular, patients with BAV-related aortopathy may show stable dilation of the ascending aorta over several years and, therefore, the frequency of repeated imaging follow-up should be individualized. On the other hand, patients with BAV and no overt aortopathy should be screened every 3 years with TTE to check for aorta dilation and additionally with repeated CT or CMR every 5 years to reconfirm TTE measurements of the aortic root and ascending aorta, as well as to reassess the arch and the descending thoracic aorta.[28]

The annual growth rate of aortic dilatation segments are significantly greater in the descending thoracic aorta, ~1.9 mm/year, than the ascending aorta, ~0.5 mm/year.[5] According to the 2014 European Society of Cardiology (ESC) guidelines, an increase >3 mm/year, confirmed by two imaging modalities, is a risk factor prompting consideration of surgical intervention in patients with a maximum diameter of 45–50 mm.[12]

The reproducibility of diameter measurements remains imperfect. Indeed, different studies have shown large inter-centre, inter-observer, and intra-observer variability for these measurements.[29] This variability is partially explained by different conventions used for measurement (how we measure the aorta) and the use of different imaging modalities and operators; for example, an increase in diameter after changing the echocardiographer is more to reflect differences in measurement technique rather than genuine disease progression.

The variability of aorta diameter measurements is typically considered to be ≤2mm.[14,30] Therefore, a real change in ascending aorta diameter, not related to measurement variability, can only be considered when greater than 2 mm. In any case, where the growth rate may impact clinical decisions, it is important to confirm any enlargement by direct side by side comparison of measurements performed on the individual sequential scans (ideally acquired by the same operator in the same centre). The use of new image registration-based semi-automatic assessment provides robust 3D mapping of aortic diameters and growth rates that go beyond the current established manual analysis and may reduce variability.[31]

Of note, any increase >3 mm by TTE should be validated by CT/CMR and compared with baseline data When follow-up is based on CT, such as the case of aortic arch and descending thoracic aorta involvement, a second modality is not necessary to confirm dilation progression. Moreover, when surgery is indicated, CT should be always performed to confirm the maximum aorta diameter as well as evaluating the coronary ostia when the aortic root is involved. At the time of surgery, TOE can also provide useful information on AV anatomy and the feasibility of AV sparing or repair surgery if aortic valvular regurgitation is present.

Post-operative aortic imaging

After any intervention on the thoracic aorta either with open or endovascular surgery, early TTE and CT or CMR are generally performed to establish a baseline reference and discard potential postoperative complications. Thereafter, annual aortic imaging is generally recommended; however, the frequency is individualized depending on patient characteristics and the type of operation performed.

Screening

About 20% of patients with thoracic aortic aneurysm or dissection have a first-degree relative with a similar disease. In familial forms, defined as more than one family member having an aortic aneurysm or dissection, aortic imaging is recommended particularly in first-degree relatives if none of the known disease-causing genes are identified.[32] If initial screening is normal, it should be repeated every 5 years until the age of 65. TTE is the primary imaging tool for screening of family members although CT or CMR is recommended at initial evaluation, to exclude the presence of aneurysms at areas poorly visualized by TTE. In sporadic cases with a high risk of genetic predisposition (<50-year-old, no hypertension in patients <60-year-old) a single screening scan in first-degree relatives may be considered. However, there are no available data on the cost-effectiveness of such an imaging screening strategy in these individuals. If the genetic cause is known, aortic imaging is performed only in carriers of the mutant gene. In the first-degree relatives of BAV patients, the prevalence of ascending aorta dilation diagnosed by TTE is around 10%; therefore, screening by TTE should be offered.[33]

Key point 5. When aortic root or ascending aorta dilation is initially diagnosed by TTE, a multiplanar CT/CMR scan is recommended to confirm TTE measurements, to rule out aortic asymmetry, and to have a baseline reference in the follow-up. When a baseline aorta diameter is >45 mm, a second exam is recommended at 6 months to confirm stability of aorta dilation, with serial exams performed on a yearly basis thereafter.

Key point 6. A genuine change in ascending aorta diameter, not related to measurement variability, can be only considered

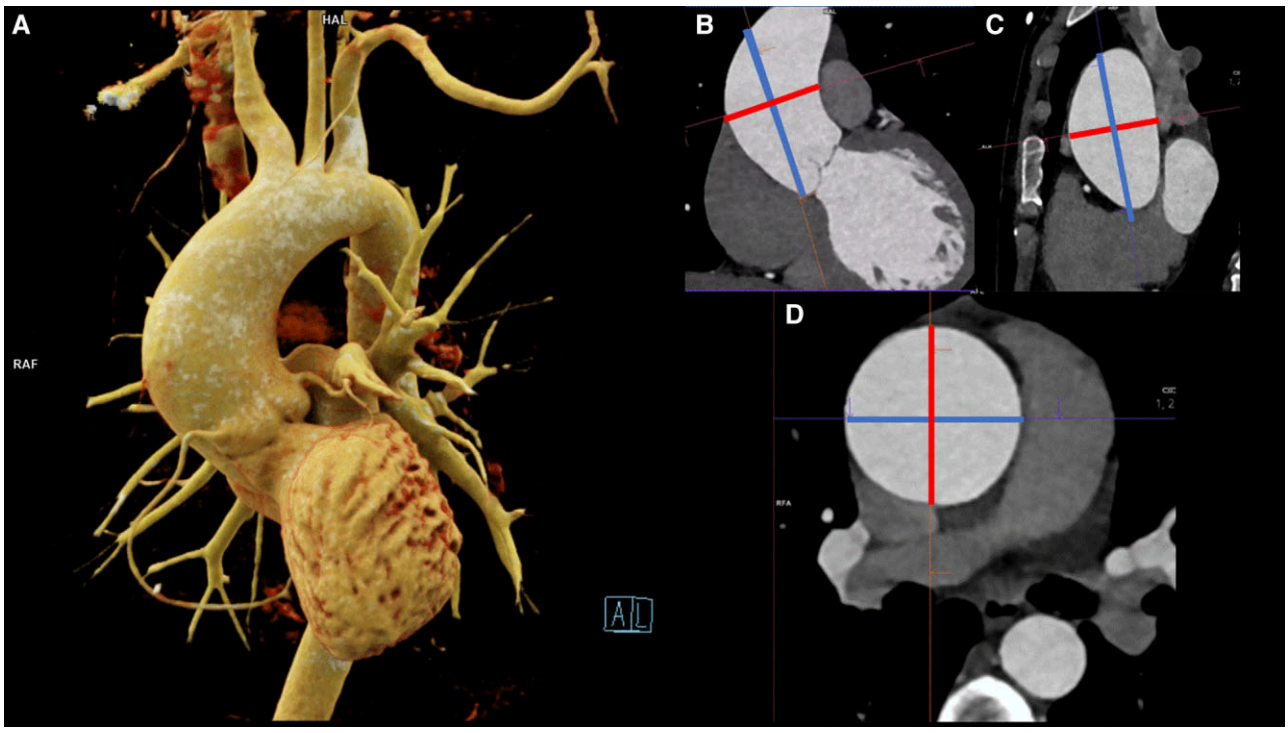

Figure 8 (*A*) Volume rendering of an ECG-gated contrast-enhanced CT angiography acquired during the diastolic phase shows a fusiform aneurysm of the ascending aorta and a normal arch. Note absence of pulse wave artefacts and motionless depiction of the coronary arteries. (*B* and *C*) Alignment of the transverse aortic plane is simultaneously performed at the most dilated location in coronal (*B*) and sagittal (*C*) multiplanar reconstructions of the ascending aorta. (*D*) The corresponding double oblique transverse multiplanar reconstruction of the ascending aorta allows for reliable and reproducible measurement of the maximum aortic distance.

when larger than 2 mm. Any increase ≥3 mm by TTE should be always validated by CT/CMR and compared with baseline data.

Acute aortic syndromes

Acute aortic syndromes (AAS) comprise a range of interrelated conditions caused by disruption of the medial layer of the aortic wall, including AD, IMH, penetrating atherosclerotic ulcer (PAU) and contained or not contained aortic aneurysm rupture. AAS are potentially life-threatening: prompt, accurate diagnosis is crucial. These clinical entities are classified as type A and type B AAS depending, respectively, on the involvement or not of the ascending aorta regardless of the site of origin (Stanford classification).[2,3,5,12,34] *Figures 9* and *10* show examples of the Stanford classification.

Aortic dissection

AD is defined as a disruption of the medial layer leading to the formation of two lumens separated by an intimomedial flap. Echocardiography, CT, and CMR can be used to diagnose AD yielding complimentary information.

Transthoracic echocardiography

TTE often provides adequate assessment of AD in the aortic root and proximal ascending aorta. While TTE can visualize most segments of the rest of the aorta (using left and right parasternal long-axis, suprasternal, apical two-chamber and subcostal scanning planes), the use of other imaging modalities is usually required in these areas. With current echo-technology and contrast enhancement, the sensitivity of TTE in the visualization of the intimal flap has improved up to ~75–85%.[35,36] Important features of AD typically include flap oscillation or motion that is independent of the aortic wall and visualized in more than one view. These features allow distinction from artefact due to reverberations from other structures. In addition, TTE provides assessment of left ventricular function, pericardial effusion, AV function, right ventricular size and function, and pulmonary artery pressure (*Figure 11*; see Supplementary data online, *Videos S3* and *S4*).

Although TTE has a lower sensitivity to diagnose type B AD, particularly in the thoracic aorta segments, the intimal flap can often be visualized in the abdominal aorta, particularly if the Nyquist level in the colour Doppler scale is lowered or contrast used. In addition, when a pleural effusion is present views from the patient's back may also be useful in identifying the flap. The low negative predictive value of TTE does not rule out AD, and further tests are required if clinical suspicion is high and the TTE examination is negative.

Transoesophageal echocardiography

The sensitivity of TOE for the diagnosis of AD reaches 99%, with a specificity of 89%.[2,3,5] Linear artefacts within the thoracic aorta on TTE and TOE can be reverberations or sidelobe artefacts. Assessing location and mobility patterns of these lineal images suggestive of reverberations of structures nearest to the transducer by M-mode is indeed key for correct interpretation, but also applying colour flow Doppler and confirmation in alternative imaging windows. Alternative modalities (CT/MR) are sometimes necessary due to dubious ultrasound artefacts, again underscoring the value of multimodality imaging in AAS. TOE is also

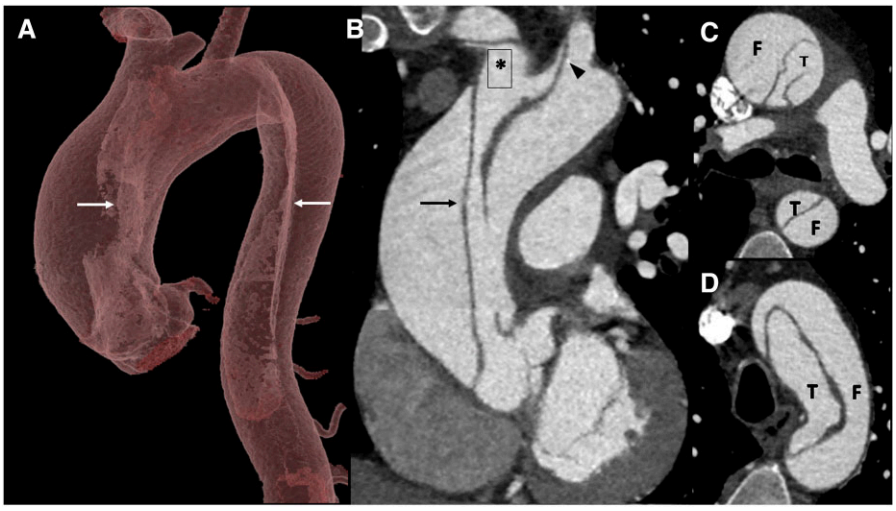

Figure 9 Classic Stanford type A aortic dissection. (*A* and *B*) Volume rendering (*A*) and oblique coronal reconstructions (*B*) show the intimal flap (*arrows*) extending from the sino-tubular junction to the aortic arch and the descending aorta, dissecting the brachiocephalic artery (*asterisk*) and the left common carotid artery (*arrowhead*). (*C* and *D*) Axial CT images show the intimal flap dividing true (*T*) and false (*F*) lumina at the level of the main pulmonary artery (*C*) and of the aortic arch (*D*). In type A aortic dissection, the false lumen is usually located along the right anterolateral wall of the ascending aorta and extends distally in a spiral fashion along the left posterolateral wall of the descending aorta.

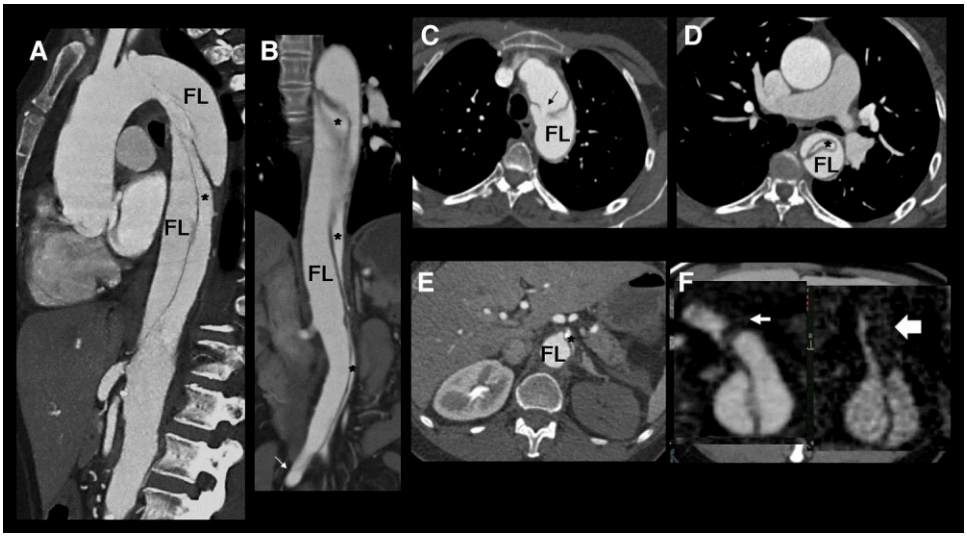

Figure 10 Acute type B aortic dissection. (*A* and *B*) Sagittal (*A*) and coronal (*B*) maximum intensity projections of an arterial phase CT angiography of an acute Stanford type B aortic dissection show the extent of the intimomedial flap from the aortic isthmus to the proximal right common iliac artery. Note the large size of the false lumen (FL) and absence of a distal entry tear (white arrow). (*C–E*) CT images show an isthmic entry tear (*C*), circumferential involvement at the retropulmonary descending thoracic aorta (*D*) with a centrally located true lumen (black asterisk) and abdominal dynamic ischemic configuration of the flap with compression of the true lumen at the ostium of the coeliac trunk (*E*) and a non-enhancing ischemic left kidney. (*F*) Multiplanar reconstructions show involvement of the coeliac trunk and the superior mesenteric artery with ischemic configuration. The flap extends into the proximal segments of both arteries, but the lack of a distal tear results in a cul-de-sac of the false lumen of the coeliac trunk (small arrow) and toral thrombosis of the FL mesenteric artery that compresses the true lumen of the visceral arteries.

very useful for locating and measuring the size of the primary entry tear and for visualizing secondary communications by colour Doppler as well as the presence of thrombus in the FL. The FL is usually larger and has less flow than the true lumen (TL). M-mode TOE shows how the intima moves towards the FL at the start of systole by expansion of the TL (*Figure 12*; see Supplementary data online, *Videos S5–S10*).

TOE is also the best technique for defining the mechanisms underlying any associated aortic valvular regurgitation. These mechanisms

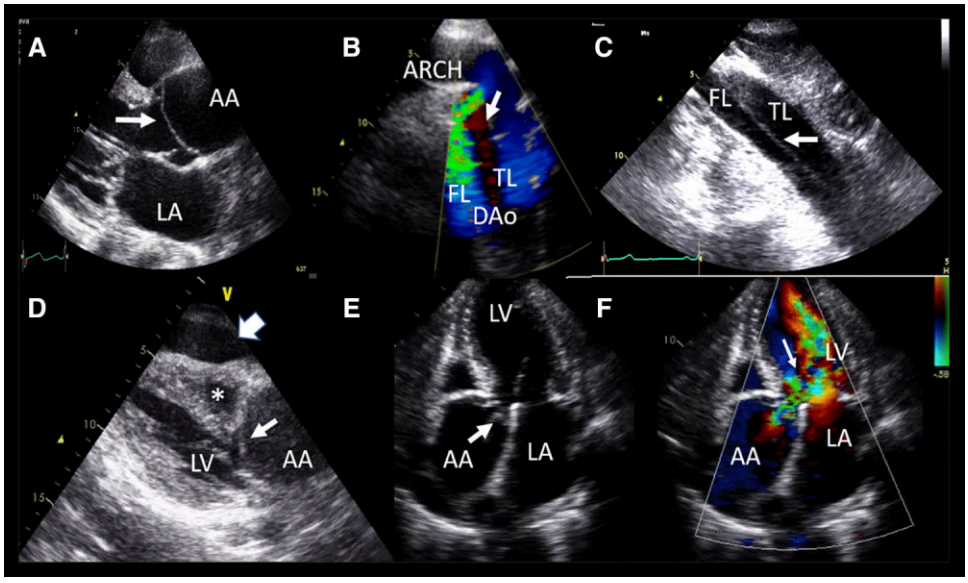

Figure 11 Aortic dissection by TTE. (*A*) Type A aortic dissection with intimal flap (arrow) in the aortic root protruding into the opening of the aortic valve by parasternal long-axis view; (*B*) type B aortic dissection with entry tear in proximal descending aorta from the suprasternal view. Arrow shows the intimal flap between false and true lumen; (*C*) abdominal aorta dissection, arrow shows the intimal flap; (*D*) pericardial tamponade (large arrow) with right ventricular (*) compression. Small arrow shows the intimal flap; (*E* and *F*) severe aortic regurgitation secondary to intimal flap prolapse into the aortic valve (arrow). AA, ascending aorta; DAo, descending aorta; FL, false lumen; LA, left atrium; LV, left ventricle; TL, true lumen. See also Supplementary data online, *Videos S3* and *S4*.

potentially include normal AV anatomy with flap invagination causing interference with valve closure, dilatation of the ascending aorta with secondary functional regurgitation, or intrinsic AV disease. TOE can differentiate two mechanisms of decreased flow in the arterial trunks in AD: proper dissection of the arterial branch, also called 'static obstruction', or alternatively, compression of the vessel ostium by the aortic intimal flap, known as 'dynamic obstruction'. Visualization of the upper abdominal aorta segment and the origins of the proximal coeliac trunk and the superior mesenteric artery should be included during the TOE assessment.[37]

3D TOE may provide additional information beyond 2D TOE allowing better morphologic and dynamic evaluation of the entry tear in AD by multiple simultaneous view.[38] In addition, contrast TOE is also very useful to better define the TL and FL, yielding a comprehensive assessment of FL flow dynamics.

The main limitation of TOE is the blind spot between the distal ascending aorta and the mid segment of the arch. Furthermore, TOE may induce gagging thereby increasing the systemic blood pressure of the patient. Adequate sedation is mandatory to avoid such reactive hypertension. Notwithstanding this precaution, we think that the systematic use of TOE to diagnose AAS should be avoided and only indicated in cases where marked haemodynamic instability precludes the safe transfer of the patient to the CT scanner or when specific information from TOE is essential. If that is the case, TOE should be always performed by an expert echocardiographer in a patient under adequate sedation or preferably a general anaesthetic. Nonetheless, TOE should be performed in the operating room in all patients during repair of type A AD. Similarly, TOE is essential to guide transcatheter endoluminal aortic repair procedures, showing the location of entry tears, secondary communications, and changes of FL flow and possible leaks after stent implantation by colour Doppler or contrast enhancement.

Computed tomography

CT is the most used imaging technique for the evaluation of AAS, particularly for AD because of its accuracy, widespread availability, and excellent sensitivity (95% for AD) providing a fast evaluation on the entire aorta and branches. Sensitivity and specificity for diagnosing arterial vessel involvement are 93% and 98%, respectively, with an overall accuracy of 96%.[2,3,12] CT can also rule out alternative causes of acute chest pain, including pulmonary embolism and coronary artery disease (*Figure 11*).

As previously described, modern CT acquisition protocols including ECG gating eliminate aortic pulsation artefacts and pseudoflaps. These protocols typically begin with a low-dose non-contrast CT to help in the detection of hyperdense IMH, followed by contrast-enhanced CT angiography. In AD, the major role of CT is to confirm the diagnosis and provide measurements of the diameter and extent of dissection, TL and FL description, involvement of organ vasculature and arterial trunks, and distance from the intimal tear to the organ arterial branches (see Supplementary data online, *Figure S1*). CT is also useful to recognize the different potential configurations of the flap when a visceral artery is involved including if the branch originates from the TL or FL, if there is flap prolapse into a branch (dynamic obstruction), or if there is intimal dissection stopping at a bifurcation (fixed obstruction) (*Figure 12*). Finally, it is also useful to diagnose visceral ischaemia, pericardial effusion and periaortic haematoma.[39] A late thoracoabdominal scan (1 min after bolus injection) distinguishes slow flow in the FL from thrombosis or IMH, improves the detection of impaired visceral perfusion, and frequently allows for alternative diagnoses in low- and intermediate-risk patients with negative AAS findings.

Cardiovascular magnetic resonance

CMR can address all issues and details of AD noninvasively with high spatial resolution and functional assessment with high sensitivity (>97%) and specificity (>94%) for diagnosing AD. However, scan times are significantly longer than for CT angiography or TOE, and monitoring of the patient during study acquisition is cumbersome. Therefore, its use in the acute phase of AAS is limited to selected cases.

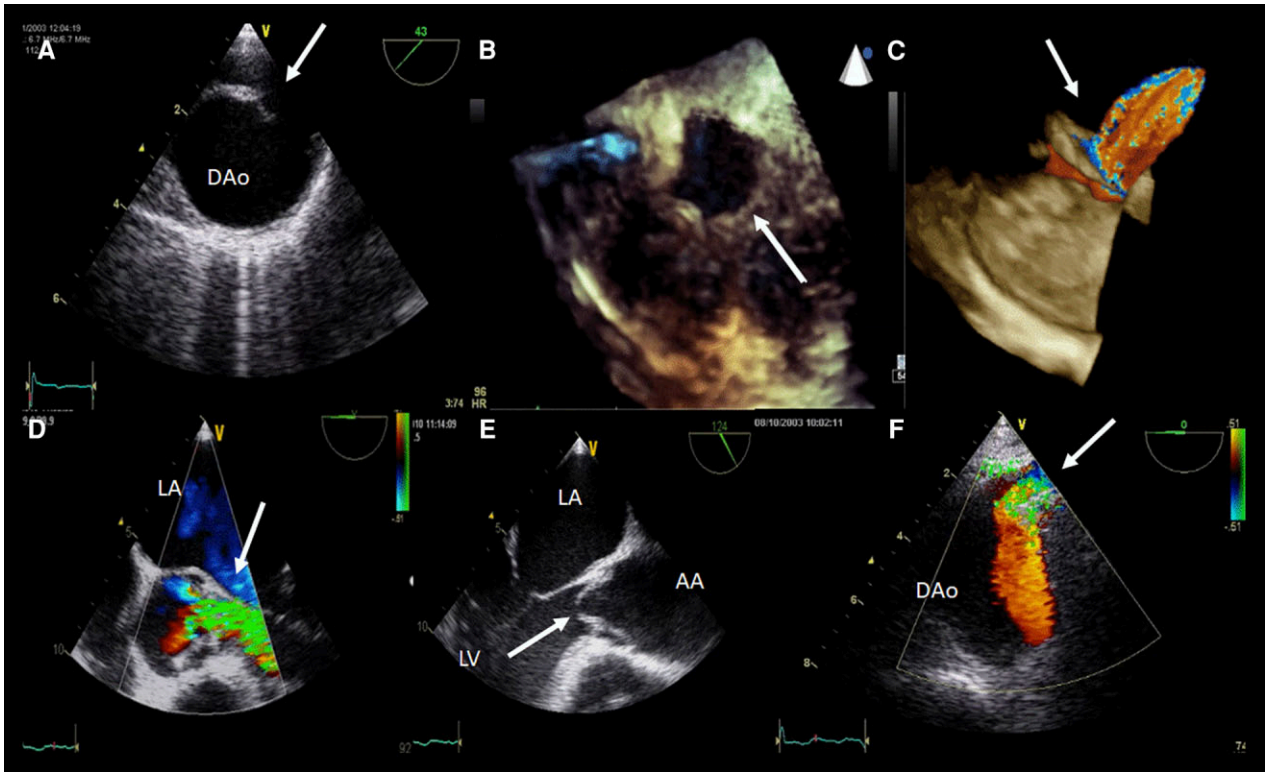

Figure 12 Transoesophageal echocardiography (TOE) in aortic dissection. (*A*) Entry tear located in proximal descending aorta by 2D TOE; (*B*) large entry tear (arrow) by 3D-TOE; (*C*) by colour Doppler, the flow of the entry tear from true to false lumen is visualized (arrow); (*D* and *E*) severe aortic regurgitation secondary to the prolapse of the flap in the left ventricular outflow tract; (*F*) dissection of the coeliac trunk with turbulent flow in the true lumen. AA, ascending aorta; DAo, descending aorta; LA, left atrium; LV, left ventricle. See also Supplementary data online, *Videos S5–S10*.

Diagnostic workup

The diagnostic workup to confirm or to rule out AD is highly dependent on the a priori risk of this condition based on three groups of variables: predisposing factors, pain characteristics, and clinical examination that are included in several proposed risk scores (*Table 1*). *Figure 13* illustrates a comprehensive diagnostic pathway. Currently, TTE is largely performed in patients with chest pain in the emergency room and maybe useful to rule out alternative diagnoses such as myocardial infarction or to detect an aortic intimal flap. Moreover, it may identify imaging signs suggestive of AAS despite not visualizing an intimal flap (pericardial effusion, aortic valvular regurgitation, aortic dilation, or aortic wall thickening).[2–5,12,39] Indeed, one of the novelties of this flow chart in comparison with previous algorithms is the suggested early implementation of TTE. A CT scan of the entire aorta should be performed in all patients with a dissection risk score >1 and increased levels of D-dimers, particularly when the troponin value is normal and there are no ECG changes suggesting myocardial ischaemia as the cause of chest pain. The exception is in patients with haemodynamic instability with high clinical suspicion or a confirmed AD on TTE who cannot be transferred to the CT scanner. In these patients, TOE should be performed under deep sedation or preferably, general anaesthesia prior to surgery.

Key point 7. TTE is currently largely performed in patients with chest pain in the emergency room and maybe useful to rule out alternative diagnoses or to detect an aortic intimal flap, particularly in the aortic root or abdominal aorta. Visualization of the intimal flap has improved with a diagnostic accuracy of ~75–85%. Special attention should be made during the TTE exam to aortic root dilatation, aortic regurgitation, and/or pericardial effusion, since these findings should raise the suspicion of AAS.

Key point 8. TOE is a reference technique in the diagnosis and assessment of thoracic AAS but, in this setting, requires adequate sedation to avoid reactive systemic arterial hypertension. When a diagnosis is definitively established using other imaging techniques, TOE should be performed preoperatively, in the operating theatre under general anaesthesia for complementary information including entry tear location and size, the mechanism underlying associated aortic regurgitation, and other associated features.

Key point 9. CT is the imaging technique of choice in the evaluation of AAS because of its accuracy, fast evaluation of the entire aorta and branches, and widespread availability. CT is very useful in the assessment of visceral organ involvement and for planning optimal therapy. The best imaging strategy for appropriately diagnosing AAS and its complications is a combination of a bedside TTE and CT.

Intramural haematoma

IMH accounts for ~10–20% of AAS. Typically, IMH appears as thickening of the aortic wall in a crescentic or concentric pattern. The aorta

Table 1 Comparison of diagnostic accuracy and pros and cons of the different imaging modalities in acute aortic syndrome

	TTE	TOE	CT	CMR
Diagnostic accuracy				
Ascending aorta dissection	++	+++	+++	+++
Aortic arch dissection	+	++	+++	+++
Descending aorta dissection	+	+++	+++	+++
Intramural haematoma	+	+++	+++	+++
Penetretating aortic ulcer	+	++	+++	+++
Aortic valve morphology and function	+++	+++	++	+++
Dynamic visualization of flap	+	+++	++	++
Aortic lumen dimensions	++	+++	+++	+++
Thrombosis of the false lumen	+	+++	+++	+++
LV, RV functional data	+++	+++	+	+++
Non-invasive haemodynamic data	+++	++	—	+
Coronary anatomy involvement	+	++	+++	++
Involvement of aortic branches	+	++	+++	+++
Pros and cons				
Ease of use	+++	++	+++	+
Portability	+++	+++	—	—
Time requirement	+	++	++	+++
Radiation	—	—	+++	—
Nephrotoxicity	—	—	++	+
Need for sedation	—	+++	—	—

lumen shape is generally preserved, and the luminal wall is curvilinear and usually smooth. This may differentiate aortic atherosclerosis and intraluminal thrombus that present more frequently with a rough, irregular border. IMH is generally a more localized process than classic AD, which typically propagates along the entire aorta towards the iliac arteries. Type A IMH may account for 30–40% of cases, whereas type B occurs in 60–70% of cases.[2,3,12]

The diagnosis of IMH is challenging and more difficult than AD. Initial imaging test results may be negative in >12% of patients; as IMH thickening may be progressive, establishing the diagnosis of IMH may require observation and repeat imaging hours or several days after the clinical onset. IMH can be difficult to distinguish from a total thrombosed FL, because they can both appear as a crescent-shaped thickening of the aorta wall. However, total thrombosis of a FL is uncommon in an initial diagnostic test and dynamic evolution is more characteristic of IMH.

For the detection of an acute IMH, TTE is generally inadequate because of low sensitivity. However, in the presence of suspicion for AAS with normal TTE, other imaging modalities are mandatory, and TOE, CT, and CMR are the main recommended modalities for the diagnosis of IMH.

The diagnostic criteria of IMH in TOE includes a wall thickness >5 mm, although in patients with severe atherosclerosis, a cut-off value >7 mm is more specific. Key features in distinguishing IMH from other pathological aortic conditions include adequate identification of the intima, which often has a bright echo-dense appearance due to calcification. Moreover, an intraparietal echo-lucent zone has been reported in 70–80% of patients with IMH. Additional signs, such as periaortic, pericardial or pleural effusion, or mediastinal haematoma, support the diagnosis of IMH and indicate overt complications in evolution (*Figure 14*).

CT without contrast is crucial for the diagnosis of IMH. A high-attenuation crescentic thickening of the aortic wall, extending in a longitudinal, non-spiral fashion, is the hallmark of this entity. In contrast to AD, the aortic lumen is rarely compromised in IMH, and no intimal flap or enhancement of the aortic wall is seen after contrast administration. Using CT, the combination of an unenhanced acquisition followed by a contrast-enhanced acquisition yields a sensitivity as high as 96% for the detection of IMH. However, in some cases, the differentiation of IMH from atherosclerotic thickening of the aorta, thrombus, or thrombosed dissection and aortitis may be difficult using CT. In those circumstances, magnetic resonance imaging (MRI) can be useful to diagnose IMH, as it offers the possibility of diagnosing intramural bleeding in the hyperacute phase because the haematoma shows an isointense signal on T1-weighted images and a hyperintense signal on T2-weighted images. Beyond the first 24 h, the change from oxyhaemoglobin to methaemoglobin determines a hyperintense signal on both T1-weighted and T2-weighted images. The differential diagnosis with mural thrombus is easier using CMR than CT or TOE, because a thrombus appears as a hypointense or isointense signal in both T1-weighted and T2-weighted sequences. Focal intimal disruption, yielding the morphologic image of ulcer-like projection of the aorta, may appear within the first days (10–30% of cases) or in the first 6 months after the acute onset of symptoms (30% of cases). Imaging predictors of complication can be also identified in the acute phase including ascending aorta involvement and maximum aortic diameter >50 mm, development of focal intimal disruption, progressive maximum wall thickness >11 mm, and haemomediastinum or progressive pleural effusion.[40]

Key point 10. IMH is diagnosed on the basis of a crescentic or circular wall thickness >5 mmm, in the clinical context of AAS. Non-contrast CT is very useful showing a high-attenuation thickening of the aortic wall. Differential diagnosis should be made with severe atherosclerosis, total thrombosis of the FL or aortitis. In doubtful cases, CMR is the technique of choice. The dynamic evolution of IMH in the acute and subacute phase requires close imaging surveillance by CT/CMR.

Penetrating atherosclerotic ulcer

A PAU is defined as an ulceration of an aortic atherosclerotic plaque penetrating through the internal elastic lamina into the media. PAU represent 2–7% of all AAS.[2,3] A real PAU must be distinguished from other 'ulcer-like' images that have been grouped under the term penetrating aortic ulcer (this term can lead to confusion given its similarity and because it can be abbreviated to the same acronym). The terms penetrating aortic ulcer or ulcer-like projections relate to an imaging morphologic concept, which include several entities of very different origin and prognosis, each of which requires diagnostic distinction from PAU.[41] *Figure 15* illustrates TOE and CT examples of PAU. PAU may occur anywhere along the length of the aorta but appears most often in the mid and distal portions of the descending thoracic aorta. Propagation of the ulcerative process may either lead to IMH, pseudoaneurysm, or even aortic rupture.

CT is the ideal diagnostic imaging modality for PAU diagnosis as it allows comprehensive visualization of the whole aorta, can identify calcified atherosclerotic plaques surrounding the ulcer, and detects extraluminal abnormalities, including pseudoaneurysms or fluid in the mediastinum or pleural space. CMR is excellent for differentiating PAU from IMH, atherosclerotic plaque, and intraluminal chronic mural thrombus.

Once developed, PAU may remain quiescent, but the weakened aortic wall may also evolve into a focal and typically saccular area of dilatation or even to an aortic pseudoaneurysm. External rupture into the mediastinum or the pleural spaces may rarely occur. Imaging predictors of complications in the acute phase are aortic maximum diameter,

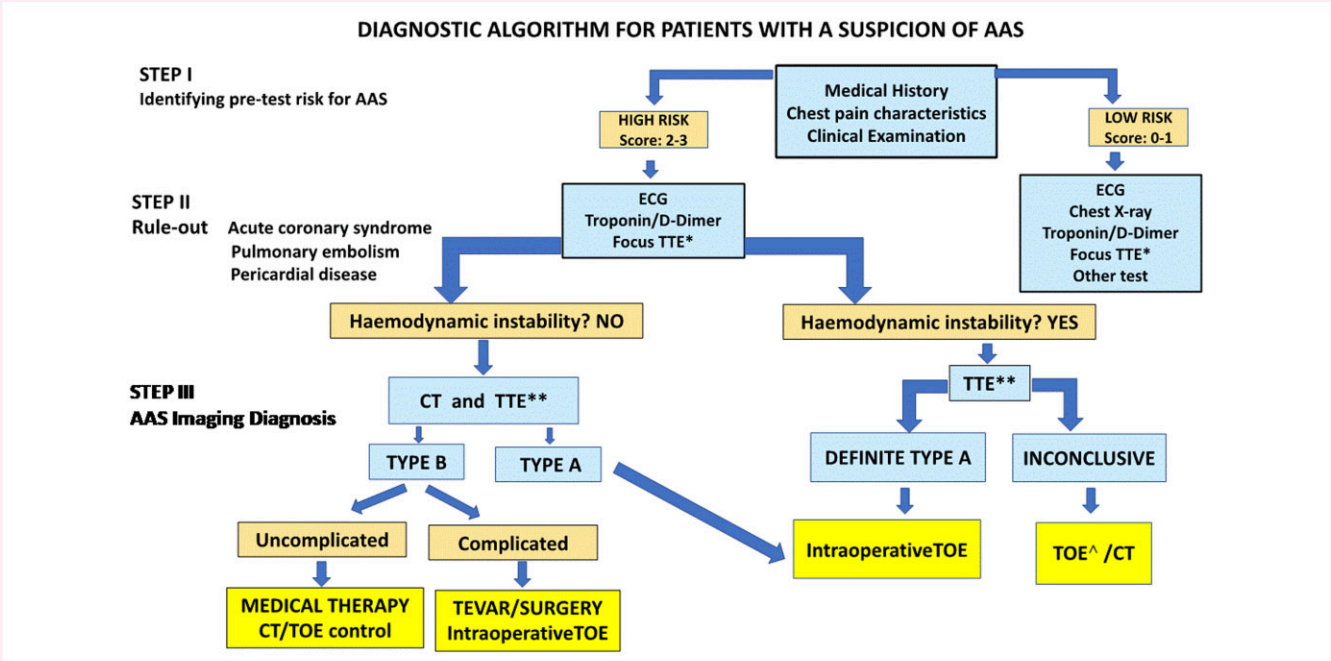

Figure 13 Diagnostic algorithm for patients with suspected acute aortic syndrome. See score description in *Table 2*. Focus TTE*: focus TTE oriented to rule out acute aortic disease, abnormal LV motion or pericardial effusion. TTE**: comprehensive TTE including evaluation of aortic valve, ventricular function, and pericardial effusion if NOT performed in Step II. ^TOE indicated only if experts in TOE are available or in patients under artificial ventilation and deep sedation/general anaesthesia.

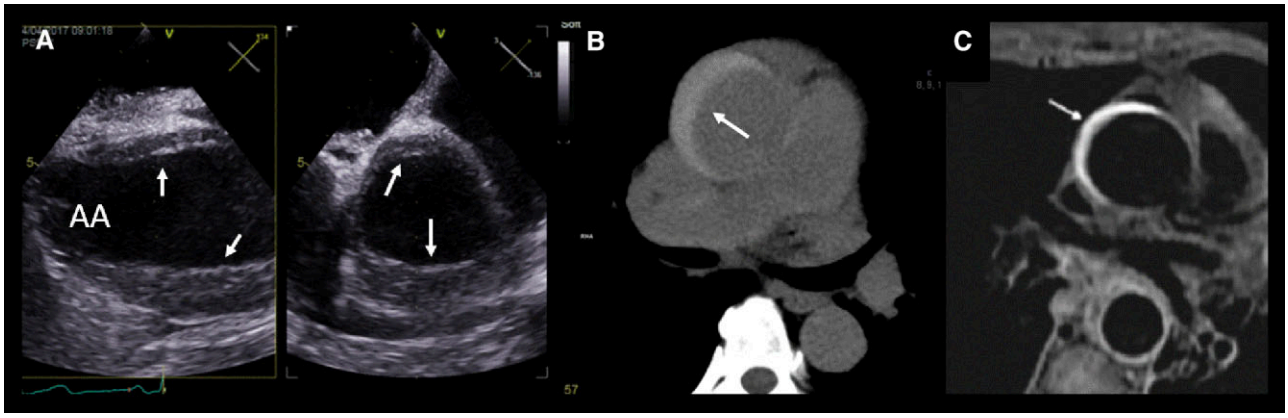

Figure 14 Intramural haematoma in ascending aorta. (*A*) Echocardiographic orthogonal views in TOE showing circumferential thickening of the aortic wall mainly in the anterior wall (arrows); (*B*) semilunar hyperattenuation (arrow) by non-contrast CT; (*C*) increased signal intensity of the aortic wall (arrow) by axial T1-weighted black-blood image in CMR.

periaortic haematoma, pleural effusion, and ulcer size. A maximum diameter >12.5 mm or an ulcer depth >9.5 mm have been reported as predictors of complications.[42]

Key point 11. The term penetrating aortic ulcer or ulcer-like projection relate to an imaging morphologic concept that includes several entities of very different origin and prognosis and that requires diagnostic distinction from a PAU. CT is the preferred imaging modality to depict it and differentiate these entities.

Aortic rupture

Rupture of the aorta is the last episode in the evolution of an aortic aneurysm or an AAS and is characterized by an acute, devastating clinical presentation that requires emergent repair whenever possible. Contained rupture commonly manifests as an aortic pseudoaneurysm (false aneurysm) defined as a dilation of the aorta due to disruption of all wall layers, which is only contained by the periaortic connective tissue. Rupture is typically diagnosed by CT with periaortic haematoma and, in some cases, identification of a discontinuity in the aortic wall with or

Table 2 Risk score for acute aortic syndrome (adapted from Ohle *et al.*[a])

	Point score	Score
Clinical history		0: Low-risk probability (< 0.5%) 1: Moderate-risk probability (0.5–5%) ≥2: High-risk probability (>5%)
• Marfan syndrome (or other connective tissue diseases) • Family history of aortic disease • Known aortic valve disease • Known thoracic aortic aneurysm • Previous aortic manipulation (including cardiac surgery)	No risk factors: 0; Any non-aneurysmal risk factors: 1; aortic aneurysm: 2	
Symptoms		
• Chest, back, or abdominal pain described as any of the following: - abrupt onset - severe intensity - ripping or tearing	No high-risk pain features: 0; 1 or 2 high-risk pain features: 1; 3 or more high-risk pain features: 2	
Clinical examination (signs)		
- Evidence of perfusion deficit: - systolic blood pressure difference - focal neurological deficit (in conjunction with pain) - pulse deficit - aortic diastolic murmur (new and with pain) - Hypotension or shock	No high-risk physical examination findings: 0; any high-risk physical examination findings: 2	

[a]Ohle R, Yan JW, Yadav K, Cournoyer A, Savage DW, Jetty P, et al. Diagnosing acute aortic syndrome: A Canadian clinical practice guideline. CMAJ 2020 Jul 20; 192: E832-E843.

without contrast extravasation (see Supplementary data online, *Figure S2*).

Traumatic and iatrogenic injury to the thoracic aorta

A variety of aortic lesions can result from blunt aortic trauma such as aortic transection, pseudoaneurysm formation, IMH, or AD. The most common location of aorta traumatic injury is at the aortic isthmus just distal to the left subclavian artery. The second most common location is the supravalvular portion of the ascending aorta. Contrast-enhanced CT is currently the preferred first-line imaging technique for blunt aortic injury, especially for patients with multiple injuries.[43] TOE and aortography might be of help when CT findings are equivocal. In some haemodynamically unstable patients, TOE may be a first-line test, especially if CT requires transportation to a remote area.

Iatrogenic injury to the thoracic aorta may occur in the setting of catheter-based interventions, during surgery or endovascular treatment. Usually, the diagnosis of this lesion is straightforward during angiography, characterized by stagnation of contrast at the level of the aortic root or ascending aorta or by the development of IMH. In this setting, IMH diagnosis requires an additional TOE or CT (see Supplementary data online, *Figure S3* and Supplementary data online, *Videos S11* and *S12*).

Advantages, limitations, and comparison among the different imaging modalities in the evaluation of AAS are summarized in *Table 2*. Because of the importance of prompt recognition to their successful treatment, this table not only emphasizes the diagnostic power of each technique but also suggests that not any single modality is preferred for all patients and that the choice of imaging modality depends on the patient's clinical condition and local institutional factors such as expertise and availability.

Imaging follow-up after AAS

As patients are still at risk of complications after an AAS, follow-up by CT or CMR is indicated depending on availability and patient characteristics at 1–3, 6, 12 months, and annually thereafter. After an ascending AD repair, complications such as local bleeding, graft infection, and pseudoaneurysm can be present. Slight fibrotic peri-graft thickening is common following surgery; however, large or asymmetrical thickening may represent localized haematoma caused by anastomotic leakage, often observed at the site of the reimplanted coronaries.

Various poor prognostic imaging signs should be considered after the acute phase of AD. A persistent patent FL in the descending thoracic aorta and a maximum aorta diameter ≥45 mm have been related to an increased growth rate[2] with a high risk of rupture if the maximum diameter is >60 mm or annual growth >5 mm.[12] A large entry tear (diameter >10 mm) in the proximal descending aorta is another established predictor of adverse events.[44] An absolute tear area difference (proximal vs. distal tears) >1.2 cm^2 has been also considered as an important risk factor.[45] However, it may be difficult to identify the distal re-entry communication; thus, in the presence of a large entry tear, indirect signs such as TL compression or partial FL thrombosis should be considered.[2] High systolic antegrade flow in the FL with significant retrograde diastolic flow assessed by 2D phase-contrast MRI identifies patients with a higher risk of complications.[46] 2D phase-contrast and 4D-flow MRI also hold promise in the functional assessment of FL flow after AD (*Figure 16*).

IMH evolution is very dynamic and may result in complete resorption with or without aorta dilation, focal intimal disruption leading to ulcer-like images, or less frequently classical AD.[47] Given their wider field of view, CMR and CT are better than TOE at defining this dynamic evolution. CMR allows monitoring of the evolution of intramural bleeding and can depict episodes of new asymptomatic intramural re-bleeding. An aorta diameter >50 mm and enlargement of focal intimal disruptions have been considered risk factors for adverse outcomes, particularly in the ascending aorta.[2,12]

Many patients with PAU do not need immediate aortic repair but do require close follow-up with serial imaging studies (by CT or CMR) to detect disease progression. In these cases, size and enlargement are the only predictors of complications and both CT and CMR are the preferred imaging modalities for follow-up.[48]

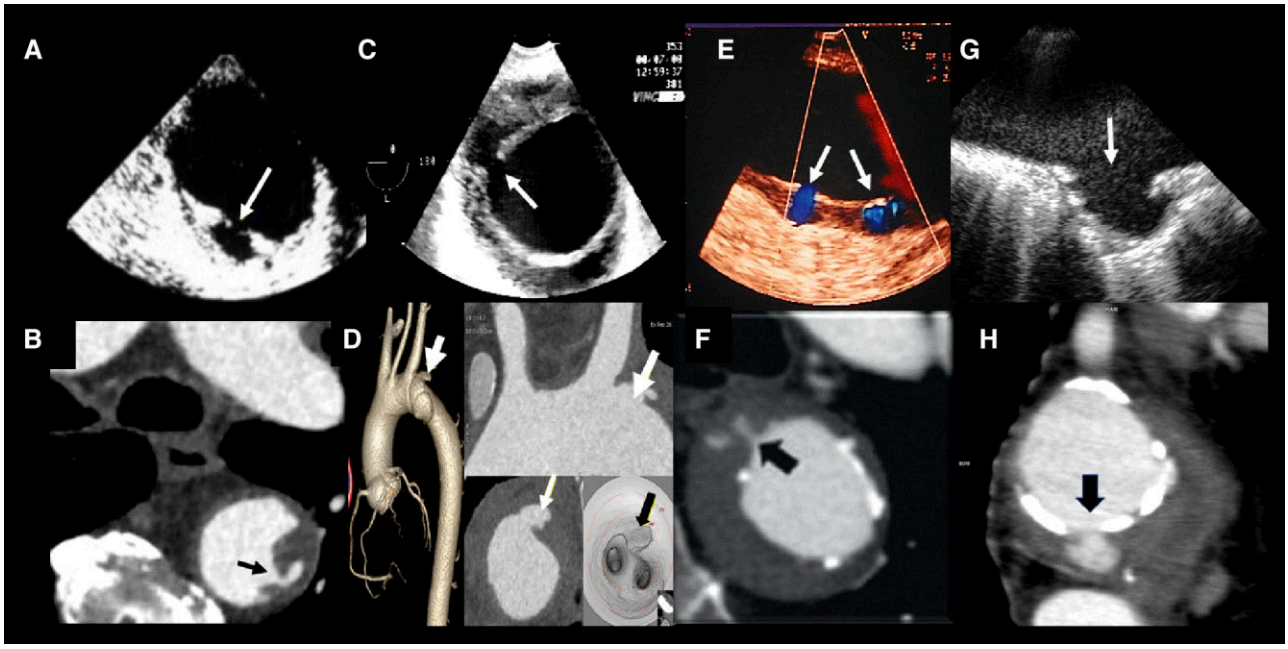

Figure 15 Different types of aortic ulcers by TOE (upper panel) and CT (lower panel). (*A* and *B*) Atherosclerotic ulcerated plaque protruding into the aorta lumen; (*C* and *D*) focal intimal disruptions (ulcer-like image) with the contrast-filled outpouching that protude from the aortic lumen into the intramural haematoma (arrows); (*E*) tiny ulcers (≤3 mm); TOE with colour Doppler may be superior to any other imaging technique for demonstrating small communications usually associated with intercostal or lumbar artery ostia (white arrows). (*F*) contrast CT may also demonstrate these small communications (black arrow); (*G* and *H*) penetrating atherosclerotic ulcer. Atherosclerotic ulcerated lesion penetrating through the aortic intima into the aortic wall with a pouch-like protrusion into the aortic wall (arrows).

Key point 12. After an AAS, follow-up by CT or CMR is indicated depending on availability and patient characteristics at 1–3, 6, 12 months, and annually thereafter. Imaging signs of poor outcome after AD include the following: a persistent patent FL in the descending thoracic aorta, maximum aorta diameter ≥45 mm, large entry tear (diameter >10 mm) in the proximal descending aorta, and a CMR FL pattern of high systolic antegrade flow with significant diastolic retrograde flow.

Key point 13. CMR is useful for monitoring the evolution of intramural bleeding and to detect new asymptomatic intramural re-bleeding episodes. Chronic and stable PAU requires close follow-up with serial imaging studies (by CT or CMR) to detect disease progression.

Aortic coarctation

Coarctation is a local narrowing of the aorta, presenting as a discrete stenosis or as a long, hypoplastic segment typically located in the area where the ductus arteriosus inserts, just distal to the subclavian artery. TTE can usually confirm the diagnosis of aortic coarctation and is used to identify associated cardiovascular disorders such as a BAV (present in >50% of patients with aortic coarctation) and aorta dilatation. Indeed, it should be always ruled out with TTE in patients with BAV or Turner syndrome due to its relatively high associated prevalence. TTE evaluation for coarctation is best done via suprasternal windows and should include colour and CW Doppler assessments of the distal arch and isthmus. Maximal velocity measurement across the coarctation by CW Doppler provides information on the severity of the stenosis but is not the only parameter to check. It is also important to determine the velocity before the stenosis and the length of the narrowed segment. When the coarctation is long or there is extensive collateral circulation, gradients might be less accurate.[49] It is important to also look for the Doppler sign of a diastolic tail in the descending thoracic aorta or the typical saw-tooth pattern of anterograde diastolic flow in the abdominal aorta because these signs indicate significant haemodynamic impairment of flow. The aortic diameter is difficult to measure and often not reliable using TTE.

CT or CMR is recommended at the time of initial evaluation to determine the site and degree of obstruction, to assess all aorta segments and the extent of collateral circulation (*Figure 17*). Pseudocoarctation can be differentiated from true coarctation by identifying a high, elongated arch, kinking that lacks luminal narrowing, and the absence of enlarged collateral arteries. Periodic follow-up by CT or CMR is also recommended after intervention to identify restenosis or progressive aorta dilation. TTE might overestimate restenosis as gradients might be high even in the absence of significant narrowing, due to decreased aorta compliance in these patients.

Key point 14. In aorta coarctation, CT or CMR is recommended at the time of initial evaluation to determine the site and degree of obstruction and to assess all aorta segments and the extent of collateral circulation. Patients with mild degrees of coarctation who do not require intervention should undergo periodic TTE (every 1–2 years) and CT or MRI (every 3–5 years) to monitor disease progression.

Aortic atherosclerosis

Atherosclerosis is characterized by the accumulation of lipids, inflammatory cells, and connective tissue cells within the arterial wall. The

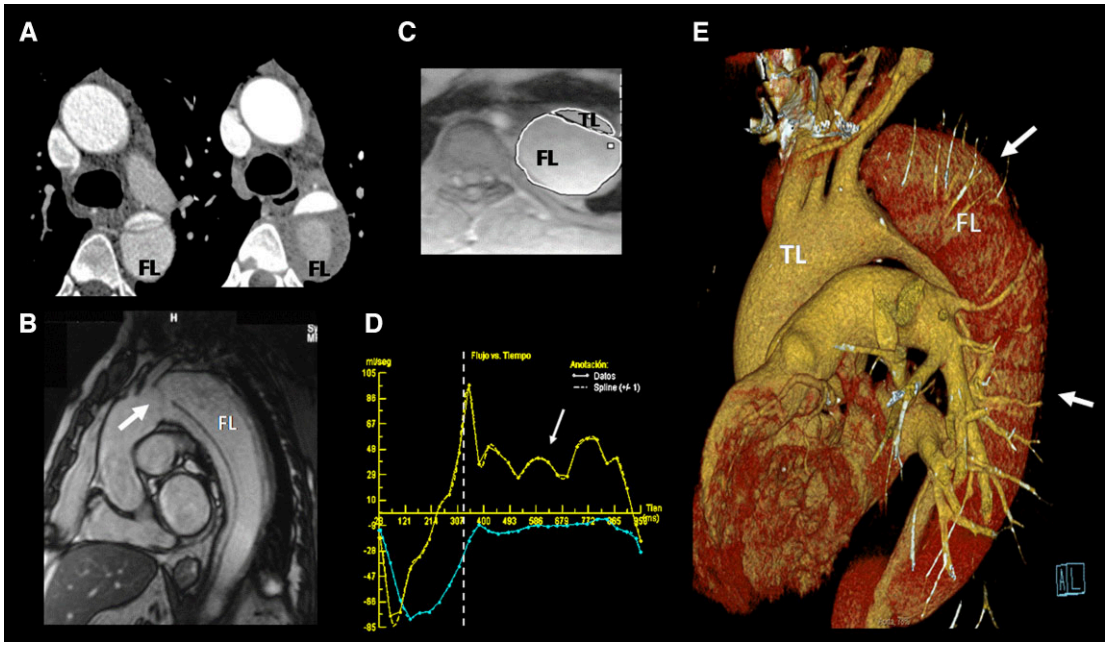

Figure 16 Outcome and predictors of type B aortic dissection. (*A*) CT images of the proximal descending thoracic aorta in the acute and chronic phases of a Stanford type B aortic dissection. Note aortic expansion caused by dilation of the hypoenhancing false lumen (FL), with the presence of partial peripheral thrombosis, indirect signs of slow flow; (*B*) descending aorta dissection with a large entry tear (arrow) by CMR; (*C*) phase-contrast gradient-echo CMR sequence for measuring the true and FL aorta flow at the inferior pulmonary level; (*D*) instantaneous flow-time curves throughout the cardiac cycle. Dotted line defines end-systole. Diastolic retrograde (arrow) flow in the FL (in yellow) is a predictor of complications; (*E*) volume-rendered image shows the characteristic hypoenhancement of the FL (arrows) and the location of the maximum aortic distance at the isthmus, close to the large entry tear.

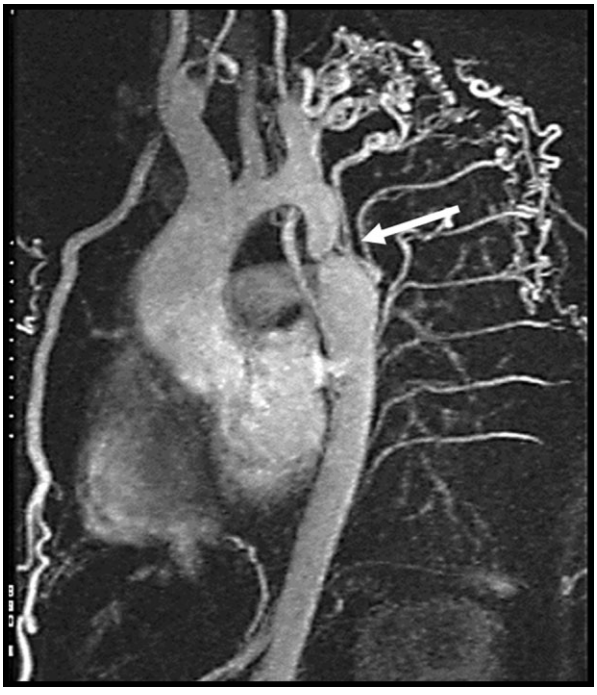

Figure 17 3D-CMR angiography of the thoracic aorta in a patient with severe aortic coarctation (arrow), showing extensive collateral vessels.

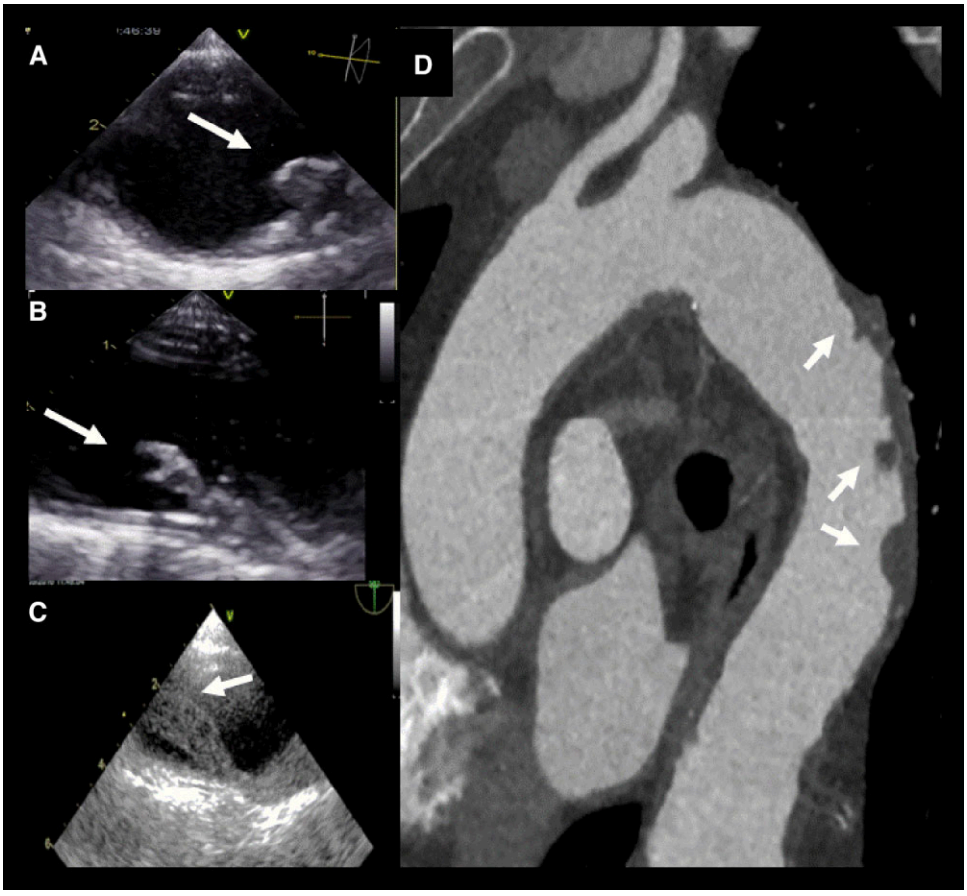

Figure 18 Atherosclerosis in descending aorta. (*A*) Atheroma with thickness >5 mm (arrow) but without any mobile element by TOE; (*B*) complex atheroma with mobile components (arrow); (*C*) large mobile thrombus defined by TOE in descending aorta (arrow); (*D*) CT angiography with diffuse atherosclerosis (arrows). See also Supplementary data online, *Videos S13* and *S14*.

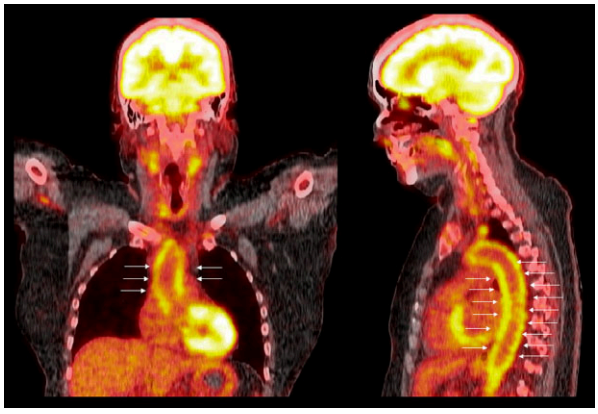

Figure 19 18F-Fluorodeoxyglucose (18F-FDG) PET/CT scan of a patient with large vessel vasculitis. High-intensity signal (arrows) is observed circumferentially around the thoracic aorta. Unpublished images provided by Jason Tarkin, Cambridge.

accumulation of fat-laden macrophages leads to thickening of the intimal layer with further progression into a mature atherosclerotic plaque. The location and characteristics of the aortic atherosclerotic burden can be partially described with TTE, but particularly TOE. TOE is the reference echocardiographic method for the evaluation of thoracic aortic atherosclerosis depicting its location (descending, arch, ascending aorta) and severity. Several classifications have been proposed to quantify severity of aortic atherosclerosis. One of the most accepted ones and recommended by this expert panel is to considered mild atherosclerosis when intimal thickening (focal or diffuse) is 2–3 mm (grade I), moderate when the atheroma thickness is <4 mm (grade II), severe when it is >4 mm (grade III), and complex when any grade has associated mobile or ulcerated components (grade IV). Mobile lesions can be (i) discrete: 1–2 mm mobile lesions, (ii) long, slender lesions that moves freely in the pulsatile flow of aorta, and (iii) a large mass that rocks with aortic blood flow. The identification of protruding atheroma ≥4 mm has been associated with stroke (*Figure 18*; see Supplementary data online, *Videos S13* and *S14*). However, TOE is less accurate in distinguish thickening, fibrosis, or calcification in the thoracic aorta than CT/CMR. Large aortic thrombi may lead to a false-positive diagnosis of dissection, particularly in the context of acute peripheral ischaemia. TEE allows accurate diagnosis and monitoring of thrombus size with time and response to anticoagulant therapy (see Supplementary data online, *Video S15*).

CT is a useful imaging modality to detect the atherosclerotic burden of thoracic aorta (*Figure 18*). Non-contrast CT is used to assess aortic calcification as a surrogate marker of the total atherosclerotic plaque burden. Contrast CT angiography allows assessment of arterial wall thickness and the burden of both calcific and non-calcific atherosclerotic plaque with high specificity for detecting aortic arch atheromas.[50] Fluorodeoxyglucose (FDG)-PET uptake provides a measure of metabolic activity and inflammation in aortic atheroma. Evaluation of thoracic aorta calcification by CT is particularly important in elderly patients undergoing cardiac surgery, in patients with previous history of radiotherapy or in in patients with previous CABG and a plan for repeat cardiac surgery.

Key point 15. Although the suprasternal window by TTE may allow identification of atherosclerotic plaques in the aortic arch, TOE permits the visualization of most thoracic aorta segments and the accurate measurement complex mobile plaques and is therefore the reference imaging modality. The severity and location of the most severe atherosclerotic plaques should be reported. CT and PET are both also useful imaging modalities to detect atherosclerotic burden and disease activity respectively in the thoracic aorta.

Aortitis

Aortitis includes all conditions leading to inflammation of the aortic wall. Imaging features include mural (inflammation, oedema, and fibrosis) and luminal alterations (dilatation/dissection, stenosis, and thrombosis). Ultimately, vessel wall hypertrophy can cause arterial stenosis and vessel occlusion. Hence, the early detection of aortitis is pivotal, facilitating identification and monitoring of the disease and the direction of appropriate therapy.

CMR, CT, and echocardiography can demonstrate homogeneous circumferential thickening of the aortic wall with a uniform smooth internal surface, which is different from the appearance of atherosclerosis but may be misdiagnosed as IMH. CT detects the characteristic aortic wall thickening observed in large vessel vasculitis as well as the vascular complications, providing a highly sensitive diagnostic technique. Black-blood CMR sequences provide similar information and may be used as an alternative although neither technique provides information on current disease activity.

18F-FDG PET/CT provides an assessment of inflammatory activity in the aorta and improves the detection of aortitis beyond CT at the segment level, detecting inflamed sections that look normal on CT and providing prognostic information.[51] In aortitis, circumferential high-intensity 18F-FDG activity is observed that can be differentiated from the more regional and lower intensity 18F-FDG uptake observed in atherosclerosis (*Figure 19*). 18F-FDG PET also holds promise in tracking disease activity with time and assessing the efficacy of glucocorticoid and immunosuppressant therapy with further research in this area required.

Key point 16. Circumferential thickening of the aortic wall on CT or CMR is a marker of aortitis. 18F-FDG PET provides an assessment of inflammation that can help establish an early diagnosis of aortitis allow monitoring of disease progression and treatment and evaluation of vascular complications and relapse.

Conclusion

Multimodality imaging plays a pivotal role in the diagnosis and management of thoracic aortic diseases. Since maximum aortic diameter is a cornerstone parameter to define evolution, prognosis and timing of intervention, the use of the recommended conventions to measure it is required to improve accuracy and reproducibility among imaging techniques. During follow-up, direct comparison of images is important to assess and detect progression of disease and evolutive changes. Measurement by echocardiography using the leading-to-leading convention and by CT/CMR using the inner-to-inner convention at end-diastole should be always adopted. In AAS, the combination of CT with TTE is the preferred and most efficient imaging strategy, while CT and CMR are the recommended ones for follow-up. Each imaging technique has strengths and limitations that should be considered before indication of a test in different clinical scenarios to answer the right clinical questions and provide essential or complementary information to apply the best care to patients with a potentially life threatening condition in the acute and chronic thoracic aortic diseases.

Supplementary material

Supplementary materials are available at *European Heart Journal - Cardiovascular Imaging* online.

Funding

None declared.

Conflict of interest: A.E.: Nothing to be declared. M.S.: Speaker and consultancy fees from Abbott (Heart Valve Disease), Edwards Lifesciences (Heart Valve Disease), Medtronic (Heart Valve Disease). Research funding from Bristol Myers Squibb (Atrial Fibrillation), Menarini (Education on Cardiovascular Diseases), Novartis (Heart Failure), Rovi (Heart Failure), Amgen (Hypercholesterolemia), Merck Sharp & Dohme (Hypercholesterolemia). V.A.: Speaker and consultancy fees from Bayer Healthcare (Antithrombotic therapies), Novo-Nordisk (Diabetes), Astrazeneca (Diabetes), Boehringer Ingelheim (Diabetes). E.B.: Nothing to be declared. H.C.: Nothing to be declared. M.R.D.: Speaker and consultancy fees from Beren, Silence Therapeutics (aortic stenosis), Jupiter Bioventures (coronary atherosclerosis), Novartis (aortic stenosis, coronary atherosclerosis), Pfizer (cardiac amyloidosis).

M.G.: Nothing to be declared. G.J.: Nothing to be declared. L.M.: Speaker and consultancy fees from Bayer (anticoagulants), Daiichi Sankyo (lipid lowering), Novartis (lipid lowering), Sanofi Aventis (lipid lowering). Research funding from Bayer (anticoagulants), Daiichi Sankyo (lipid lowering),

Novartis (lipid lowering), Sanofi Aventis (lipid lowering). R.N.: Speaker and consultancy fees from Bayer and Sanofi Genzyme. Research funding from Biotronik and Philips Volcano. M.P.: Nothing to be declared. G.P.: Nothing to be declared. J.R.-P.: Speaker and consultancy fees from Pfizer (Amyloidosis), Takeda Pharmaceuticals (Fabry disease), Amicus (Fabry disease). Research funding from General Electric and Circle Cardiovascular Imaging, Inc (Advanced cardiac imaging).

J.W.R.-H.: Nothing to be declared. R.v.K.: Speaker and consultancy fees from Novartis (heart failure), Sanofi Aventis (heart failure), Bayer Netherlands (heart failure). Research funding from Novartis (heart failure).

Data availability

No new data were generated or analysed in support of this research. This is a review consensus paper, and the data presented are related to the corresponding references inserted throughout the text.

References

1. Lang RM, Badano LP, Mor-Avi V, Afilalo J, Armstrong A, Ernande L *et al.* Recommendations for cardiac chamber quantification by echocardiography in adults: an update from the American Society of Echocardiography and the European Association of Cardiovascular Imaging. *Eur Heart J Cardiovasc Imaging* 2015;**16**:233–70.
2. Goldstein SA, Evangelista A, Abbara S, Arai A, Asch FM, Badano LP *et al.* Multimodality imaging of diseases of the thoracic aorta in adults: from the American Society of Echocardiography and the European Association of Cardiovascular Imaging: endorsed by the Society of Cardiovascular Computed Tomography and Society for Cardiovascular Magnetic Resonance. *J Am Soc Echocardiogr* 2015;**28**:119–82.
3. Evangelista A, Flachskampf FA, Erbel R, Antonini-Canterin F, Vlachopoulos C, Rocchi G *et al.* Echocardiography in aortic diseases: EAE recommendations for clinical practice. *Eur J Echocardiogr* 2010;**11**:645–58.
4. Ali SG, Fusini L, Dalla Cia A, Tamborini G, Gripari P, Muratori M *et al.* Technological advancements in echocardiographic assessment of thoracic aortic dilatation: head to head comparison among multidetector computed tomography, 2-dimensional, and 3-dimensional echocardiography measurements. *J Thorac Imaging* 2018;**33**:232–9.
5. Flachskampf FA, Wouters PF, Edvardsen T, Evangelista A, Habib G, Hoffman P *et al.* Recommendations for transoesophageal echocardiography: EACVI update 2014. *Eur Heart J Cardiovasc Imaging* 2014;**15**:353–65.
6. Wu W, Budovec J, Foley WD. Prospective and retrospective ECG gating for thoracic CT angiography: a comparative study. *Am J Roentgenol* 2009;**193**:955–63.
7. Leiner T, Bogaert J, Friedrich MG, Mohiaddin R, Muthurangu V, Myerson S *et al.* SCMR Position Paper (2020) on clinical indications for cardiovascular magnetic resonance. *J Cardiovasc Magn Reson* 2020;**22**:76–113.
8. Guala A, Rodriguez-Palomares J, Dux-Santoy L, Teixido-Tura G, Maldonado G, Galian L *et al.* Influence of aortic dilation on the regional aortic stiffness of bicuspid aortic valve assessed by 4-dimensional flow cardiac magnetic resonance: comparison with Marfan syndrome and degenerative aortic aneurysm. *JACC Cardiovascular Imaging* 2019;**12**:1020–9.
9. Mohiaddin RH, Kilner PJ, Rees S, Longmore DB. Magnetic resonance volume flow and jet velocity mapping in aortic coarctation. *J Am Coll Cardiol* 1993;**22**:1515–21.
10. Burris NS, Hope MD. 4D flow MRI applications for aortic disease. *Magn Reson Imaging Clin N Am* 2015;**23**:15–23.
11. Dweck MR, Aikawa E, Newby DE, Tarkin JM, Rudd JHF, Narula J *et al.* Noninvasive molecular imaging of disease activity in atherosclerosis. *Circ Res* 2016;**119**:330–40.
12. Erbel R, Aboyans V, Boileau C, Bossone E, Bartolomeo RD, Eggebrecht H *et al.* 2014 ESC guidelines on the diagnosis and treatment of aortic diseases: document covering acute and chronic aortic diseases of the thoracic and abdominal aorta of the adult. *Eur Heart J* 2014;**35**:2873–926.
13. Muraru D, Maffessanti F, Kocabay G, Peluso D, Bianco LD, Piasentini E *et al.* Ascending aorta diameters measured by echocardiography using both leading edge-to-leading edge and inner edge-to-inner edge conventions in healthy volunteers. *Eur Heart J Cardiovasc Imaging* 2014;**15**:415–22.
14. Rodríguez-Palomares JF, Teixidó-Tura G, Galuppo V, Cuéllar H, Laynez A, Gutiérrez L *et al.* Multimodality assessment of ascending aortic diameters: comparison of different measurement methods. *J Am Soc Echocardiogr* 2016;**29**:819–26.e4.
15. Saura D, Dulgheru R, Caballero L, Bernard A, Kou S, Gonjilashvili N *et al.* Two-dimensional transthoracic echocardiographic normal reference ranges for proximal aorta dimensions: results from the EACVI NORRE study. *Eur Heart J Cardiovasc Imaging* 2017;**18**:167–79.
16. Amsallem M, Ou P, Milleron O, Henry-Feugeas MC, Detaint D, Arnoult F *et al.* Comparative assessment of ascending aortic aneurysms in Marfan patients using ECG-gated computerized tomographic angiography versus trans-thoracic echocardiography. *Int J Cardiol* 2015;**184**:22–7.
17. Bons LR, Duijnhouwer AL, Boccalini S, van den Hoven AT, van der Vlugt MJ, Chelu RG *et al.* Intermodality variation of aortic dimensions: how, where and when to measure the ascending aorta. *Int J Cardiol* 2019;**276**:230–5.
18. van Hout MJ, Scholte AJ, Juffermans JF, Westenberg JJ, Zhong L, Zhou X *et al.* How to measure the aorta using MRI: a practical guide. *J Magn Reson Imaging* 2020;**52**:971–7.
19. Vis JC, Rodríguez-Palomares JF, Teixidó-Tura G, Galian-Gay L, Granato C, Guala A *et al.* Implications of asymmetry and valvular morphotype on echocardiographic measurements of the aortic root in bicuspid aortic valve. *J Am Soc Echocardiogr* 2019;**32**:105–12.
20. Plonek T, Berezowski M, Bochenek M, Filip G, Rylski B, Golesworthy T *et al.* A comparison of aortic root measurements by echocardiography and computed tomography. *J Thorac Cardiovasc Surg* 2019;**157**:479–86.
21. Campens L, Demulier L, de Groote K, Vandekerckhove K, de Wolf D, Roman MJ *et al.* Reference values for echocardiographic assessment of the diameter of the aortic root and ascending aorta spanning all age categories. *Am J Cardiol* 2014;**114**:914–20.
22. Pham MHC, Ballegaard C, de Knegt MC, Sigvardsen PE, Sørgaard MH, Fuchs A *et al.* Normal values of aortic dimensions assessed by multidetector computed tomography in the Copenhagen General Population Study. *Eur Heart J CardiovascImaging* 2019;**20**:939–48.
23. Burman ED, Keegan J, Kilner PJ. Aortic root measurement by cardiovascular magnetic resonance: specification of planes and lines of measurement and corresponding normal values. *Circ Cardiovasc Imaging* 2008;**1**:104–13.
24. Davis AE, Lewandowski AJ, Holloway CJ, Ntusi NAB, Banerjee R, Nethononda R *et al.* Observational study of regional aortic size referenced to body size: production of a cardiovascular magnetic resonance nomogram. *J Cardiovasc Magn Reson* 2014;**16**:9–18.
25. Milleron O, Arnoult F, Delorme G, Detaint D, Pellenc Q, Raffoul R *et al.* Pathogenic FBN1 genetic variation and aortic dissection in patients with Marfan syndrome. *J Am Coll Cardiol* 2020;**75**:843–53.
26. Franken R, El Morabit A, de Waard V, Timmermans J, Scholte AJ, van den Berg MP *et al.* Increased aortic tortuosity indicates a more severe aortic phenotype in adults with Marfan syndrome. *Int J Cardiol* 2015;**194**:7–12.
27. Lopez-Sainz A, Mila L, Rodriguez-Palomares J, Limeres J, Granato C, la Mura L *et al.* Aortic branch aneurysms and vascular risk in patients with Marfan syndrome. *J Am Coll Cardiol* 2021;**77**:3005–12.
28. Borger MA, Fedak PWM, Stephens EH, Gleason TG, Girdauskas E, Ikonomidis JS *et al.* The American Association for Thoracic Surgery consensus guidelines on bicuspid aortic valve–related aortopathy: full online-only version. *J Thorac Cardiovasc Surg* 2018;**156**:e41–74.
29. Asch FM, Yuriditsky E, Prakash SK, Roman MJ, Weinsaft JW, Weissman G *et al.* The need for standardized methods for measuring the aorta multimodality core lab experience from the GenTAC Registry. *JACC: Cardiovascular Imaging* 2016;**9**:219–26.
30. Quint LE, Liu PS, Booher AM, Watcharotone K, Myles JD. Proximal thoracic aortic diameter measurements at CT: repeatability and reproducibility according to measurement method. *Int J Cardiovasc Imaging* 2013;**29**:479–88.
31. Dux-Santoy L, Rodríguez-Palomares JF, Teixidó-Turà G, Ruiz-Muñoz A, Casas G, Valente F *et al.* Registration-based semi-automatic assessment of aortic diameter growth rate from contrast-enhanced computed tomography outperforms manual quantification. *Eur Radiol* 2022;**32**:1997–2009.
32. Mariscalco G, Debiec R, Elefteriades JA, Samani NJ, Murphy GJ. Systematic review of studies that have evaluated screening tests in relatives of patients affected by nonsyndromic thoracic aortic disease. *J Am Heart Assoc* 2018;**7**:e009302.
33. Galian-Gay L, Carro Hevia A, Teixido-Turà G, Rodríguez Palomares J, Gutiérrez-Moreno L, Maldonado G *et al.* Familial clustering of bicuspid aortic valve and its relationship with aortic dilation in first-degree relatives. *Heart* 2019;**105**:603–8.
34. Neskovic AN, Hagendorff A, Lancellotti P, Guarracino F, Varga A, Cosyns B *et al.* Emergency echocardiography: the European Association of Cardiovascular Imaging recommendations. *Eur Heart J Cardiovasc Imaging* 2013;**14**:1–11.
35. Cecconi M, Chirillo F, Costantini C, Iacobone G, Lopez E, Zanoli R *et al.* The role of transthoracic echocardiography in the diagnosis and management of acute type A aortic syndrome. *Am Heart J* 2012;**163**:112–8.
36. Evangelista A, Avegliano G, Aguilar R, Cuellar H, Igual A, González-Alujas T *et al.* Impact of contrast-enhanced echocardiography on the diagnostic algorithm of acute aortic dissection. *Eur Heart J* 2010;**31**:472–9.
37. Moral S, Avegliano G, Cuéllar H, Ballesteros E, Rodríguez-Palomares J, Teixidó G *et al.* Usefulness of transesophageal echocardiography in the evaluation of celiac trunk and superior mesenteric artery involvement in acute aortic dissection. *J Am Soc Echocardiogr* 2021;**34**:327–35.
38. Evangelista A, Aguilar R, Cuellar H, Thomas M, Laynez A, Rodrguez-Palomares J *et al.* Usefulness of real-time three-dimensional transoesophageal echocardiography in the assessment of chronic aortic dissection. *Eur J Echocardiogr* 2011;**12**:272–7.
39. Vardhanabhuti V, Nicol E, Morgan-Hughes G, Roobottom CA, Roditi G, Hamilton MCK *et al.* Recommendations for accurate CT diagnosis of suspected acute aortic syndrome (AAS)-on behalf of the British Society of Cardiovascular Imaging (BSCI)/British Society of Cardiovascular CT (BSCCT). *Br J Radiol* 2016;**89**:20150705.
40. Moral S, Cuéllar H, Avegliano G, Ballesteros E, Salcedo MT, Ferreira-González I *et al.* Clinical implications of focal intimal disruption in patients with type B intramural hematoma. *J Am Coll Cardiol* 2017;**69**:28–39.

41. Evangelista A, Moral S, Ballesteros E, Castillo-Gandía A. Beyond the term penetrating aortic ulcer: a morphologic descriptor covering a constellation of entities with different prognoses. *Prog Cardiovasc Dis* 2020;**63**:488–95.
42. Yang L, Zhang QY, Wang XZ, Zhao X, Liu XZ, Wang P *et al.* Long-term imaging evolution and clinical prognosis among patients with acute penetrating aortic ulcers: a retrospective observational study. *J Am Heart Assoc* 2020;**9**:e014505.
43. Patel NR, Dick E, Batrick N, Jenkins M, Kashef E. Pearls and pitfalls in imaging of blunt traumatic thoracic aortic injury: a pictorial review. *Br J Radiol* 2018;**91**:20180130.
44. Evangelista A, Salas A, Ribera A, Ferreira-González I, Cuellar H, Pineda V *et al.* Long-term outcome of aortic dissection with patent false lumen: predictive role of entry tear size and location. *Circulation* 2012;**125**:3133–41.
45. Cuellar-Calabria H, Burcet G, Roque A, Rodríguez-Palomares J, Teixidó G, Rodríguez R *et al.* Differences in the area of proximal and distal entry tears at CT angiography predict long-term clinical outcomes in aortic dissection. *Radiol Cardiothorac Imaging* 2021;**3**: e210029.
46. Evangelista A, Pineda V, Guala A, Bijnens B, Cuellar H, Rudenick P *et al.* False lumen flow assessment by magnetic resonance imaging and long-term outcomes in uncomplicated aortic dissection. *J Am Coll Cardiol* 2022;**79**:2415–27.
47. Evangelista A, Dominguez R, Sebastia C, Salas A, Permanyer-Miralda G, Avegliano G *et al.* Long-term follow-up of aortic intramural hematoma: predictors of outcome. *Circulation* 2003;**108**:583–9.
48. Carroll BJ, Schermerhorn ML, Manning WJ. Imaging for acute aortic syndromes. *Heart* 2019;**106**:182–9.
49. Dijkema EJ, Leiner T, Grotenhuis HB. Diagnosis, imaging and clinical management of aortic coarctation. *Heart* 2017;**103**:1148–55.
50. Cohen A, Donal E, Delgado V, Pepi M, Tsang T, Gerber B *et al.* EACVI recommendations on cardiovascular imaging for the detection of embolic sources: endorsed by the Canadian Society of Echocardiography. *Eur Heart J Cardiovasc Imaging* 2021;**22**:e24–57.
51. Hartlage GR, Palios J, Barron BJ, Stillman AE, Bossone E, Clements SD *et al.* Multimodality imaging of aortitis. *JACC: Cardiovasc Imaging* 2014;**7**:605–19.